Vertical propagation of non-hydrostatic gravity waves into the mesosphere

Andreas Dörnbrack & MA Team[1]

Piotr K. Smolarkiewicz[2] and Ulrich Schumann[1]

[1]DLR Oberpfaffenhofen

Institut für Physik der Atmos

[2]ECMWF Reading

- Goals
- Methods
- Selected Cases
  - o Auckland RF23
  - o RF05

DEEPWAVE Meeting, Yale University, New Haven, CT, 8 August 2017

Status of DEEPWAVE-related Publications

Gisinger, S., A. Dörnbrack, V. Matthias, J. D. Doyle, S. D. Eckermann, B. Ehard, L. Hoffmann, B. Kaifler, C. G. Kruse, and M. Rapp, 2017: Atmospheric Conditions during the Deep Propagating Gravity Wave Experiment (DEEPWAVE), *Mon. Wea. Rev*., EOR: https://doi.org/10.1175/MWR-D-16-0435.1

Kaifler, N., Kaifler, B., Ehard, B., Gisinger, S., Dörnbrack, A., Rapp, M.,Kivi, R., Kozlovsky, A., Lester, M., and Liley, B., 2017: Observational indications of downward-propagating gravity waves in middle atmosphere lidar data, *Journal of Atmospheric and Solar-Terrestrial Physics*, EOR: https://doi.org/10.1016/j.jastp.2017.03.003

Ehard, B., B. Kaifler, A. Dörnbrack, P. Preusse, S. D. Eckermann, M. Bramberger, S. Gisinger, N. Kaifler, B. Liley, J. Wagner, and M. Rapp, 2017: Horizontal propagation of large-amplitude mountain waves into the polar night jet, *J. Geophys. Res. Atmos.*, **122**, 1423–1436, doi:10.1002/2016JD025621.

Witschas, B., S. Rahm, A. Dörnbrack, J. Wagner, and M. Rapp, 2017: Airborne Coherent Doppler Wind Lidar measurements of vertical and horizontal winds for the investigation of orographically induced gravity waves. *J. Atmos. Oceanic Technol*., **34**, 1371–1386, https://doi.org/10.1175/JTECH-D-17-0021.1

Dörnbrack, A., S. Gisinger, and B. Kaifler, 2017: On the interpretation of gravity wave measurements by ground-based lidars, *Atmosphere,* ***8****, 1–22. DOI: 10.3390/atmos8030049 ISSN 2073-443.*

Dörnbrack, A., S. Gisinger, M. C. Pitts, L. R. Poole, and M. Maturilli, 2017: Multilevel cloud structure over Svalbard, *Mon. Wea. Rev*., **145**, 1149–1159, doi: 10.1175/MWR-D-16-0214.1.

Wagner, J., Dörnbrack, A., Rapp, M., Gisinger, S., Ehard, B., Bramberger, M., Witschas, B., Chouza, F., Rahm, S., Mallaun, C., Baumgarten, G., and Hoor, P., 2017: Observed versus simulated mountain waves over Scandinavia – improvement of vertical winds, energy and momentum fluxes by enhanced model resolution?, *Atmos. Chem. Phys*., **17**, 4031-4052, doi:10.5194/acp-17-4031-2017.

Status of DEEPWAVE-related Publications

Submitted and in Review:

Portele, T. C., A. Dörnbrack, B. & N. Kaifler, J. S. Wagner, P.-D. Pautet, and M. Rapp, 2017: Mountain Wave Propagation under Transient Tropospheric Forcing: A DEEPWAVE Case Study. *Mon. Wea. Rev*., revisions submitted his week.

Heller, R., C. Voigt, S. Kaufmann, A. Dörnbrack, J. Wagner, H. Schlager, S. Beaton, K. Young, and M. Rapp, 2017: Mountain waves modulate the water vapour distribution in the UTLS, submitted to *Atmos. Chem. Phys*., 10 April, 2017; accepted with minor revisions.

Bramberger, M., A. Dörnbrack, K. Bossert, B. Ehard, D. C. Fritts, B. Kaifler, C. Mallaun, A. Orr, P.-D. Pautet, M. Rapp, M. J. Taylor, S. Vosper, B. Williams, and B. Witschas, 2017: Does strong tropospheric forcing cause large-amplitude mesospheric gravity waves? - A DEEPWAVE Case Study. *J. Geophys. Res*., submitted 27 June 2017

Ehard, B., S. Malardel, A. Dörnbrack, B. Kaifler, N. Kaifler, and N. Wedi, 2017: Comparing ECMWF high resolution analyses to lidar temperature measurements in the middle atmosphere. submitted to *Q. J. R. Met. Soc*. 16 April 2017

Krisch, I., Preusse, P., Ungermann, J., Dörnbrack, A., Eckermann, S. D., Ern, M., Friedl-Vallon, F., Kaufmann, M., Oelhaf, H., Rapp, M., Strube, C., and Riese, M., 2017: First tomographic observations of gravity waves by the infrared limb imager GLORIA, *Atmos. Chem. Phys. Discuss*., https://doi.org/10.5194/acp-2017-644, in review.

Associated Publication:

Giez, A., Mallaun, C., Zöger, M., Dörnbrack, A., and Schumann, U., 2017: Static Pressure from Aircraft Trailing-Cone Measurements and Numerical Weather-Prediction Analysis. *Journal of Aircraft*. DOI: 110.2514/1.C034084 ISSN 0021-8669

Goals

- quasi-realistic numerical simulations of the flow across NZ and Auckland Islands from the surface to the mesosphere @ about 100 km
- understanding of the vertical propagation under
  - o different forcing conditions in the troposphere
  - o different stratospheric conditions for propagation
- compare with linear dynamics by conducting quasi-linear‘ simulations
- try to reproduce the observed ‚broad spectra‘ and to understand the processes causing them

Methods

- 2D (later 3D) numerical simulations with EULAG (multiscale geophysical flow solver) integrating different approximations of the Navier-Stokes equations:

  o compressible , pseudo-incompressible, anelastic, linearized versions

  o inviscid

  o lateral wave absorber

  o vertical: exponentially increasing Rayleigh friction

- realistic topography along the mountain transects Mt Aspiring and Mt. Cook (taken from GV-data set)

- initial wind, potential temperature, density profiles:

  o ECMWF IFS up to 80 km altitude

  o NAVGEM up to 100 km altitude

Auckland Case RF23 14 July 2014

Dynamics of Orographic Gravity Waves Observed in the Mesosphere over the Auckland Islands during the Deep Propagating Gravity Wave Experiment (DEEPWAVE)

STEPHEN D. ECKERMANN,[a] DAVE BROUTMAN,[b] JUN MA,[b] JAMES D. DOYLE,[c] PIERRE-DOMINIQUE PAUTET,[d] MICHAEL J. TAYLOR,[d] KATRINA BOSSERT,[e] BIFFORD P. WILLIAMS,[e] DAVID C. FRITTS,[e] AND RONALD B. SMITH[f]

[a] *Space Science Division, U.S. Naval Research Laboratory, Washington, D.C.*
[b] *Computational Physics, Inc., Springfield, Virginia*
[c] *Marine Meteorology Division, U.S. Naval Research Laboratory, Monterey, California*
[d] *Center for Atmospheric and Space Sciences, Utah State University, Logan, Utah*
[e] *GATS, Inc., Boulder, Colorado*
[f] *Department of Geology and Geophysics, Yale University, New Haven, Connecticut*

Eckermann, S., D. Broutman, J. Ma, J. Doyle, P. Pautet, M. Taylor, K. Bossert, B. Williams, D. Fritts, and R. Smith, 2016: Dynamics of Orographic Gravity Waves Observed in the Mesosphere over the Auckland Islands during the Deep Propagating Gravity Wave Experiment (DEEPWAVE). *J. Atmos. Sci.,* 73, 3855–3876, doi: 10.1175/JAS-D-16-0059.1.

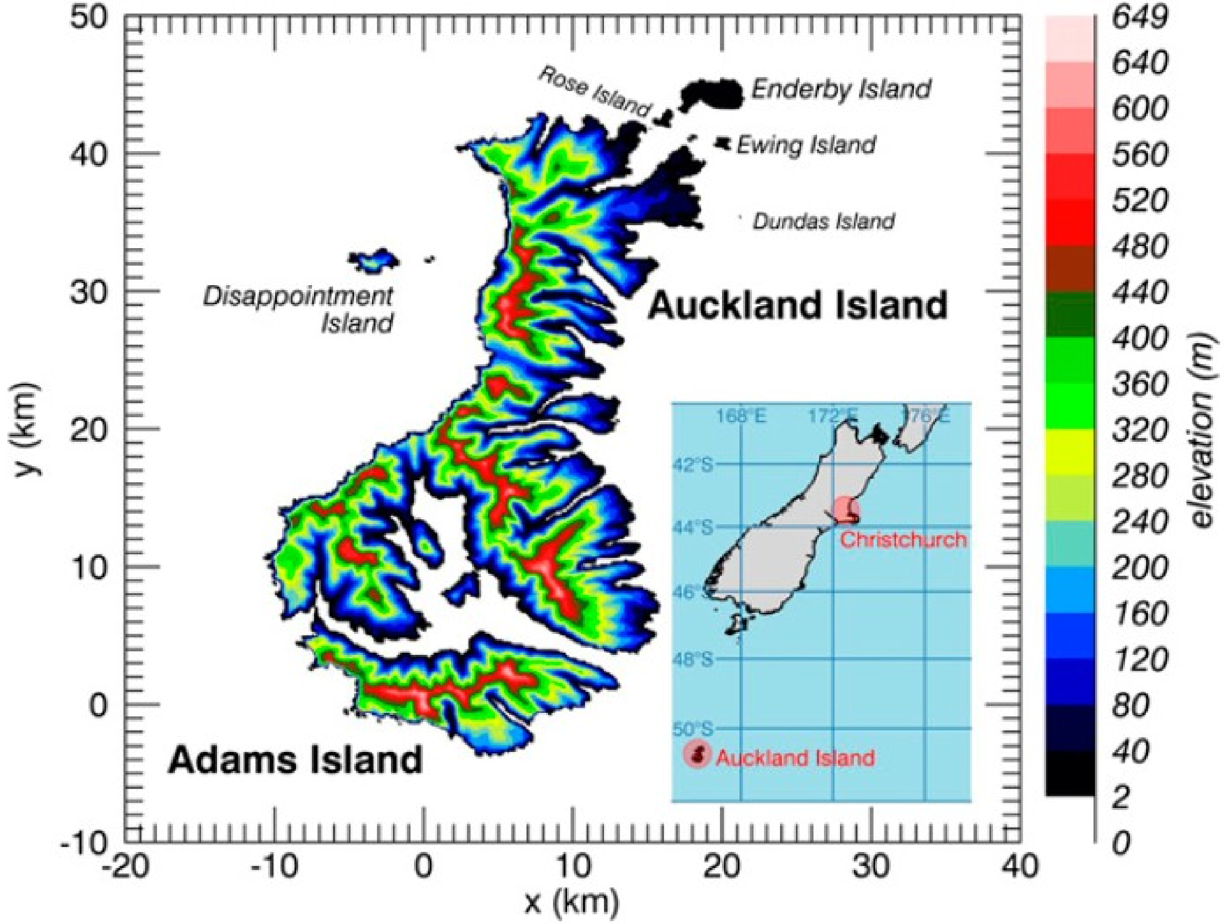

FIG. 1. Terrain elevations $h(x, y)$ of the Auckland Island archipelago derived from ASTER observations (see section 2c). Origin of (x, y) coordinate axes is located at Mount Dick, the highest peak. (inset) Map showing location of Auckland Island relative to DEEPWAVE operating base in Christchurch, New Zealand.

Eckermann, S., D. Broutman, J. Ma, J. Doyle, P. Pautet, M. Taylor, K. Bossert, B. Williams, D. Fritts, and R. Smith, 2016: Dynamics of Orographic Gravity Waves Observed in the Mesosphere over the Auckland Islands during the Deep Propagating Gravity Wave Experiment (DEEPWAVE). *J. Atmos. Sci.,* 73, 3855–3876, doi: 10.1175/JAS-D-16-0059.1.

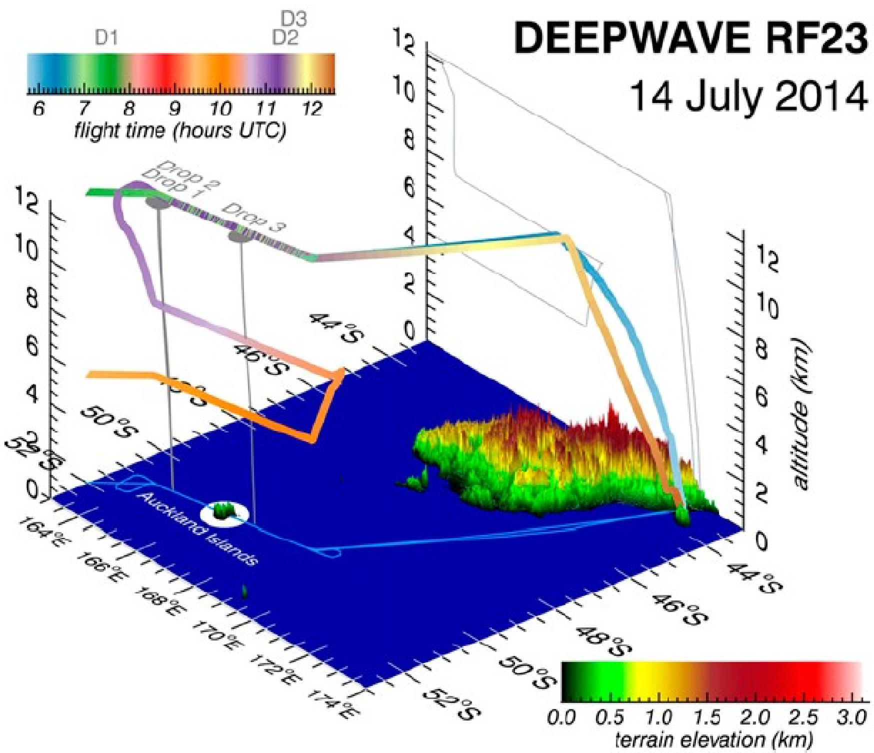

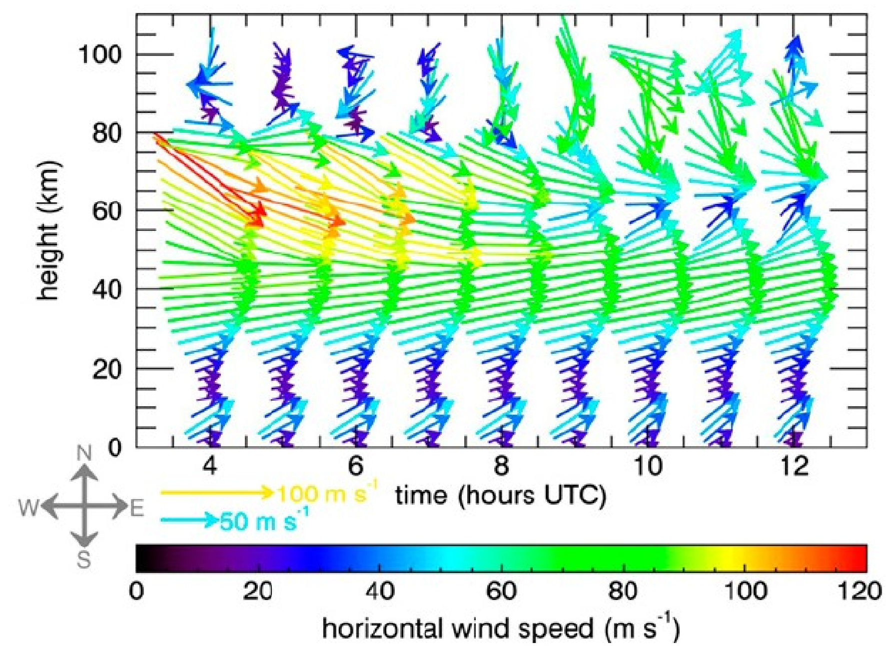

FIG. 4. Horizontal wind vectors upstream of Auckland Island on 14 Jul 2014 from NAVGEM reanalysis, plotted at hourly intervals from 0400 to 1200 UTC over the range z = 0–100 km.

Eckermann, S., D. Broutman, J. Ma, J. Doyle, P. Pautet, M. Taylor, K. Bossert, B. Williams, D. Fritts, and R. Smith, 2016: Dynamics of Orographic Gravity Waves Observed in the Mesosphere over the Auckland Islands during the Deep Propagating Gravity Wave Experiment (DEEPWAVE). *J. Atmos. Sci.,* 73, 3855–3876, doi: 10.1175/JAS-D-16-0059.1.

Observations at ~ 80 km altitude 14 July 2014

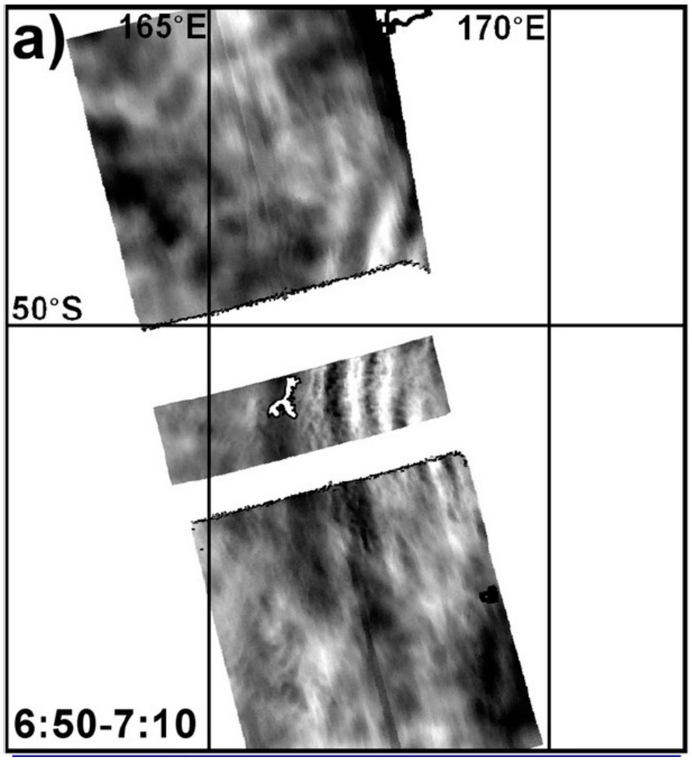

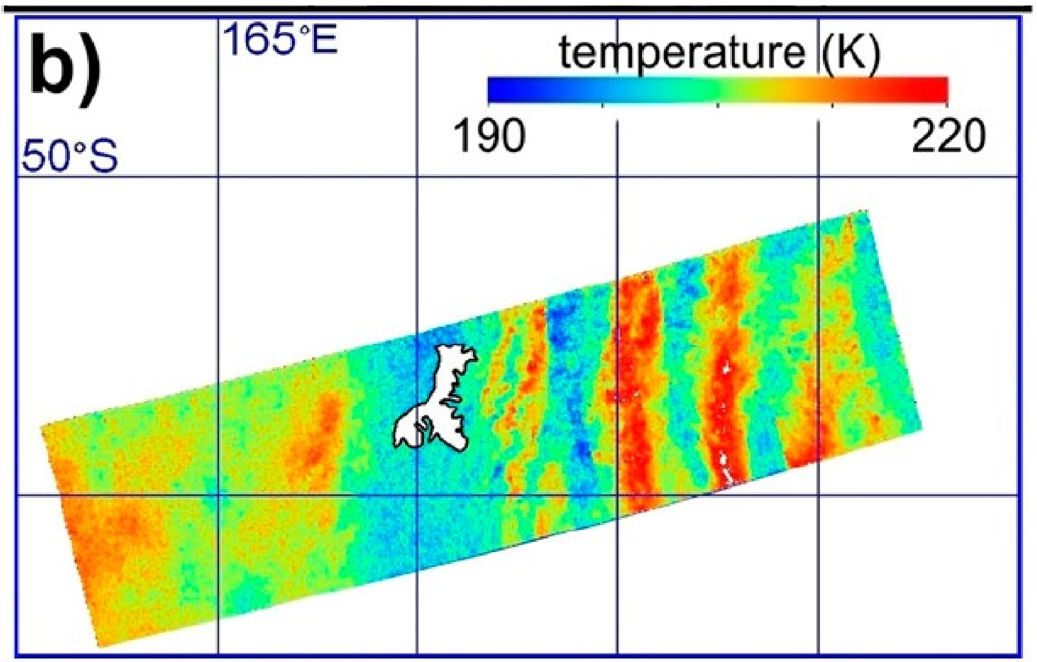

FIG. 5. (a) OH airglow brightness from the AMTM zenith and wing cameras during the first outbound NGV transect. Auckland Island is shaded white with the coastline outlined in black. Time span of these observations (UTC) is indicated at bottom left of this panel. (b) Rotational temperatures retrieved from the zenith camera airglow brightness in (a). See text and Pautet et al. (2016) for further details.

Eckermann, S., D. Broutman, J. Ma, J. Doyle, P. Pautet, M. Taylor, K. Bossert, B. Williams, D. Fritts, and R. Smith, 2016: Dynamics of Orographic Gravity Waves Observed in the Mesosphere over the Auckland Islands during the Deep Propagating Gravity Wave Experiment (DEEPWAVE). *J. Atmos. Sci.*, 73, 3855–3876, doi: 10.1175/JAS-D-16-0059.1.

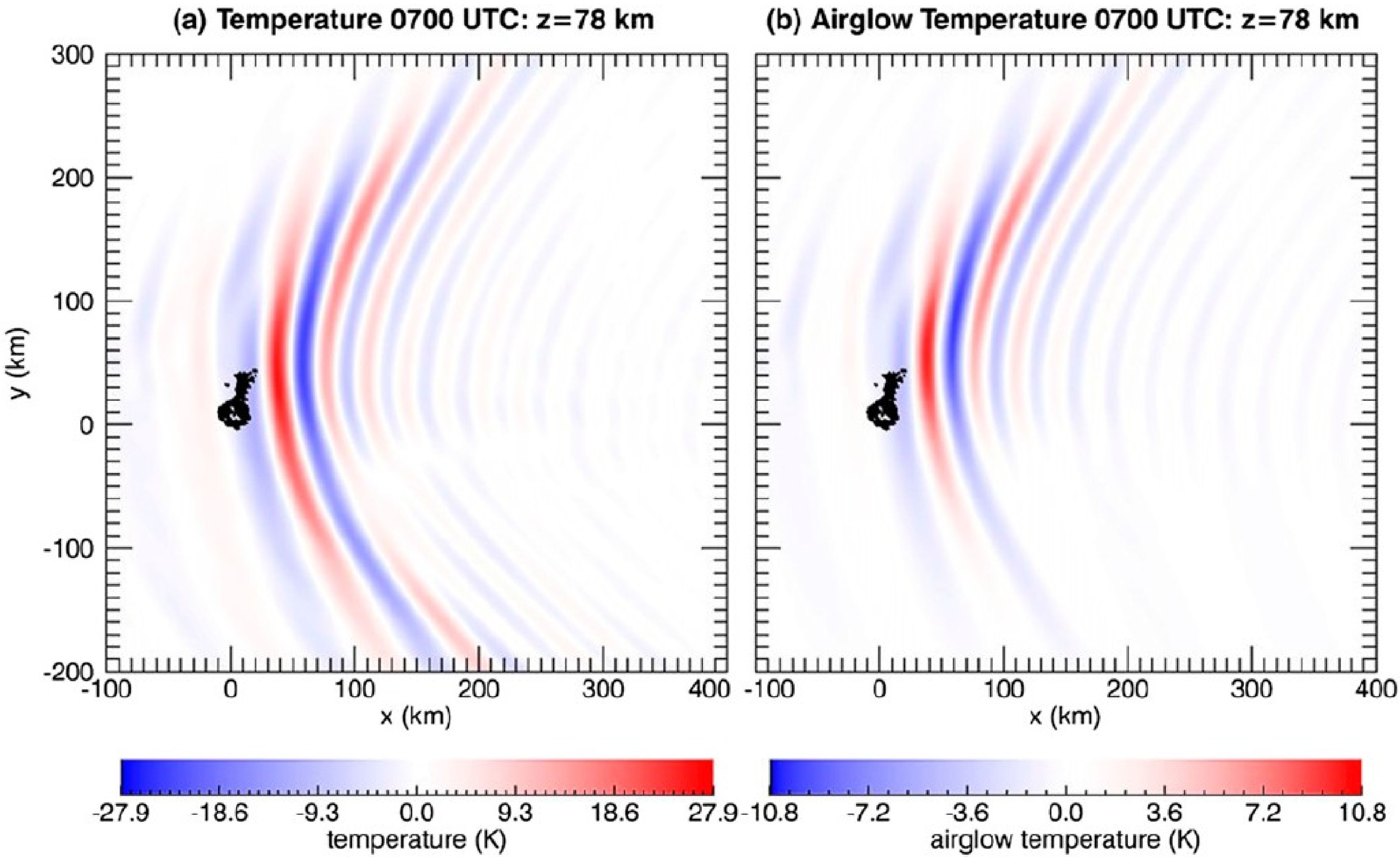

FIG. 11. (a) $T'(x, y, z, t_c)$ Fourier solution (K; color bar) at $z = 78$ km and $t_c = 4$ h, calculated using NAVGEM background profiles at 0700 UTC. (b) Modified solutions after applying the airglow filter function $S_{AG}(m)$ in (17) via (3).

Eckermann, S., D. Broutman, J. Ma, J. Doyle, P. Pautet, M. Taylor, K. Bossert, B. Williams, D. Fritts, and R. Smith, 2016: Dynamics of Orographic Gravity Waves Observed in the Mesosphere over the Auckland Islands during the Deep Propagating Gravity Wave Experiment (DEEPWAVE). *J. Atmos. Sci.,* 73, 3855–3876, doi: 10.1175/JAS-D-16-0059.1.

Vertical Profiles 14 July 2014 06 UTC

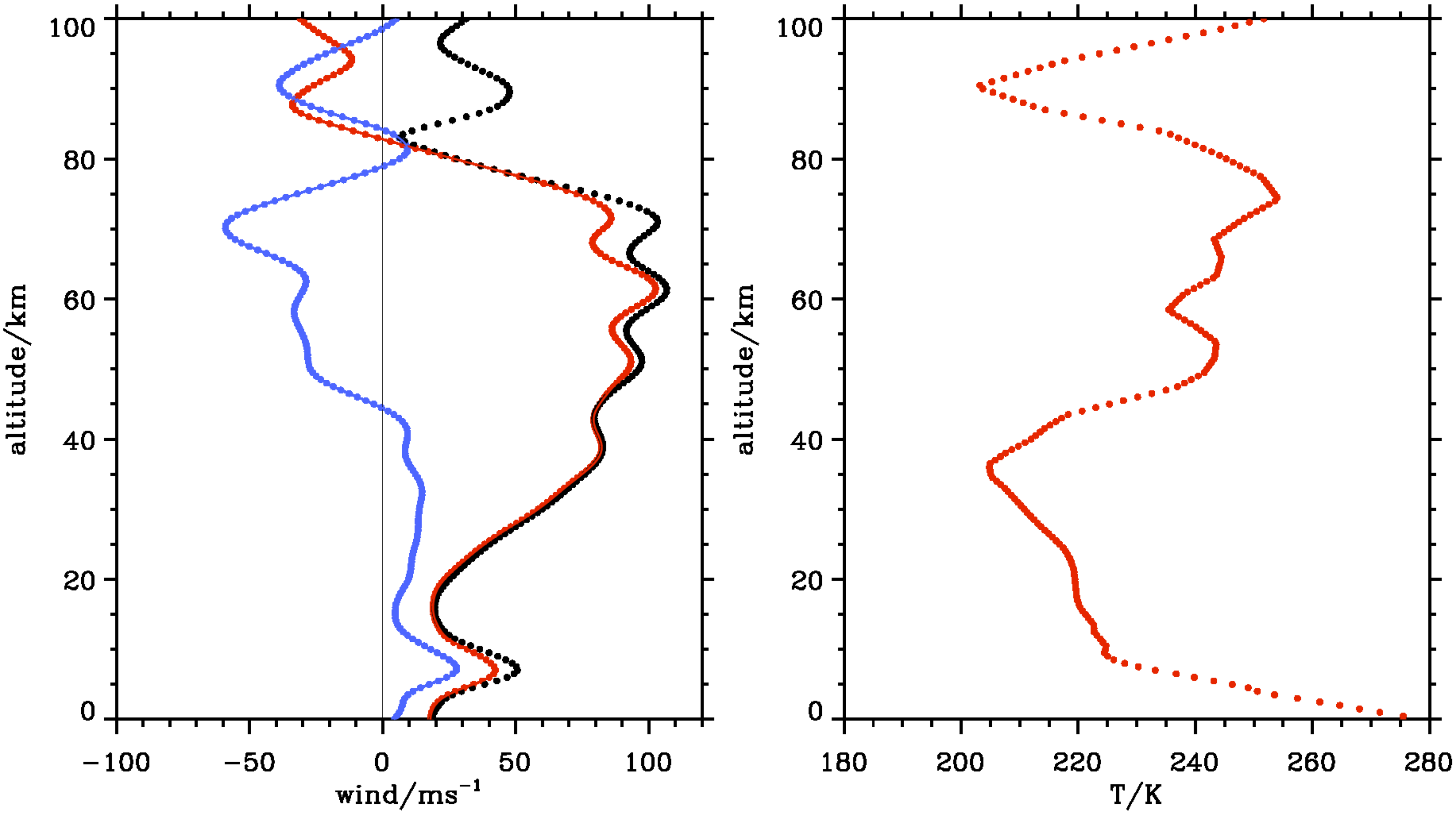

meridional component
zonal component
horizontal wind

Vertical Profiles 14 July 2014 06 UTC

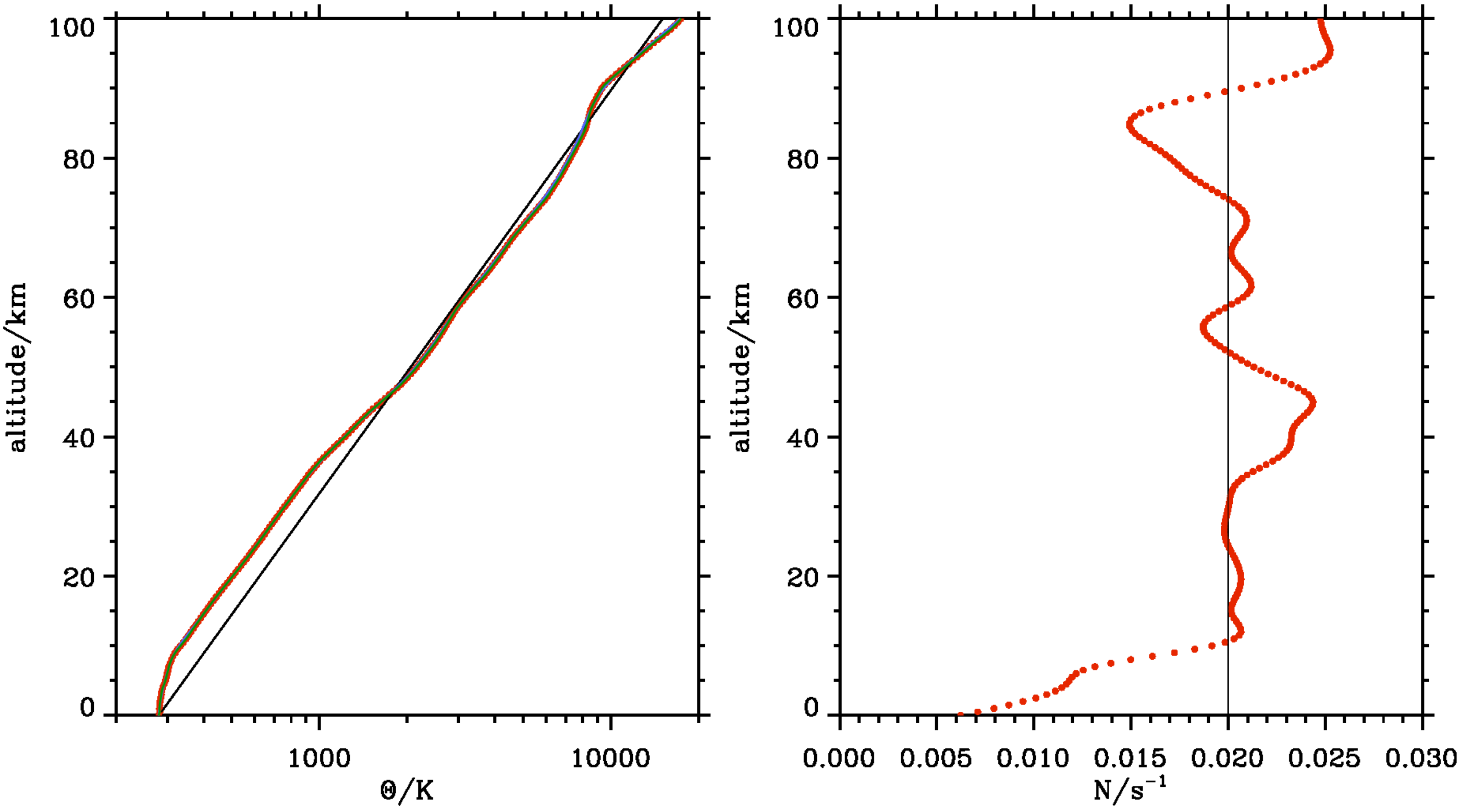

Advanced Spaceborne Thermal Emission and Reflection Radiometer (ASTER) Terrain Elevation

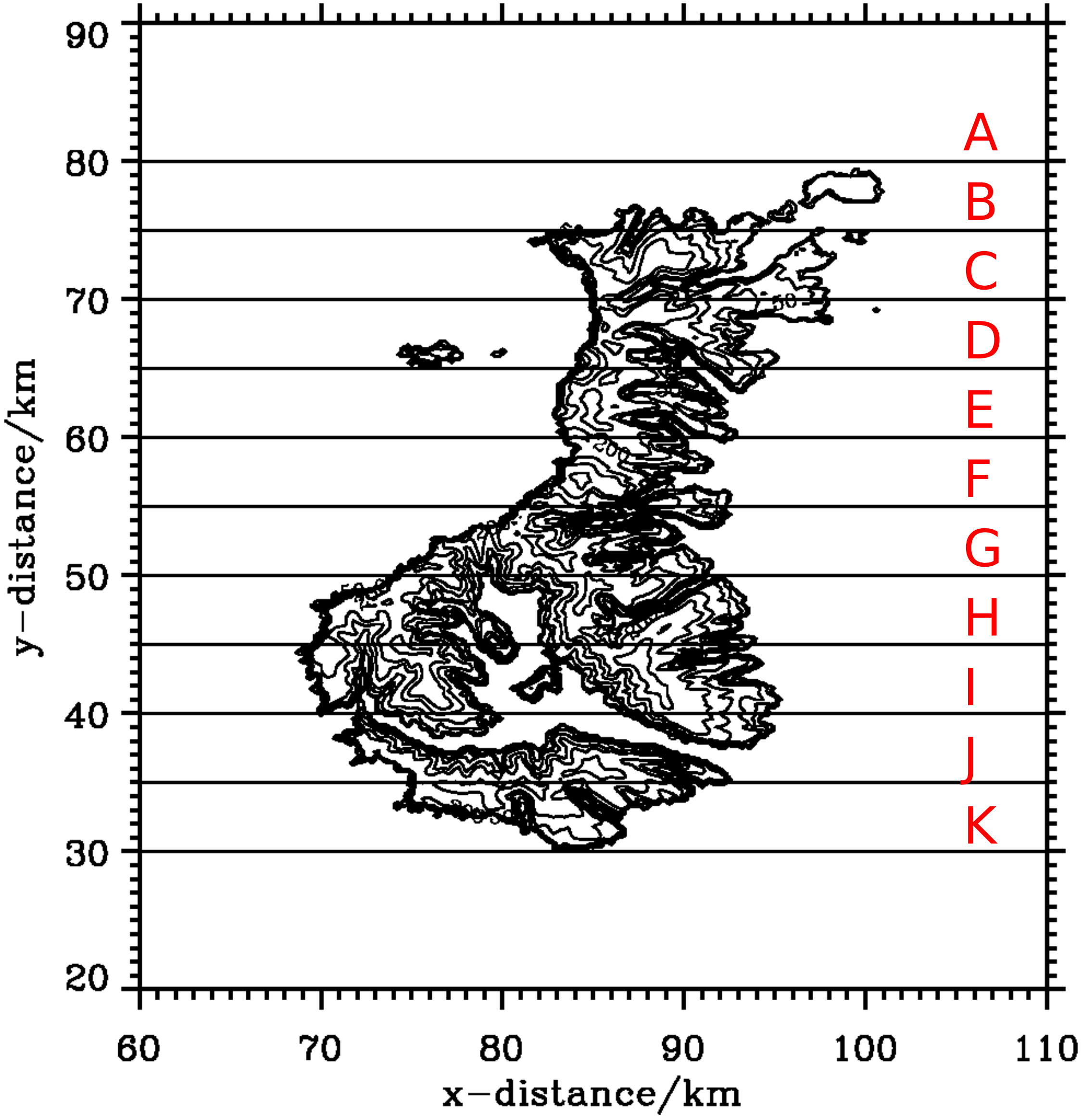

200 m horizontal resolution from the ASTER (on NASA's Terra satellite) global digital elevation model

Section G (250)

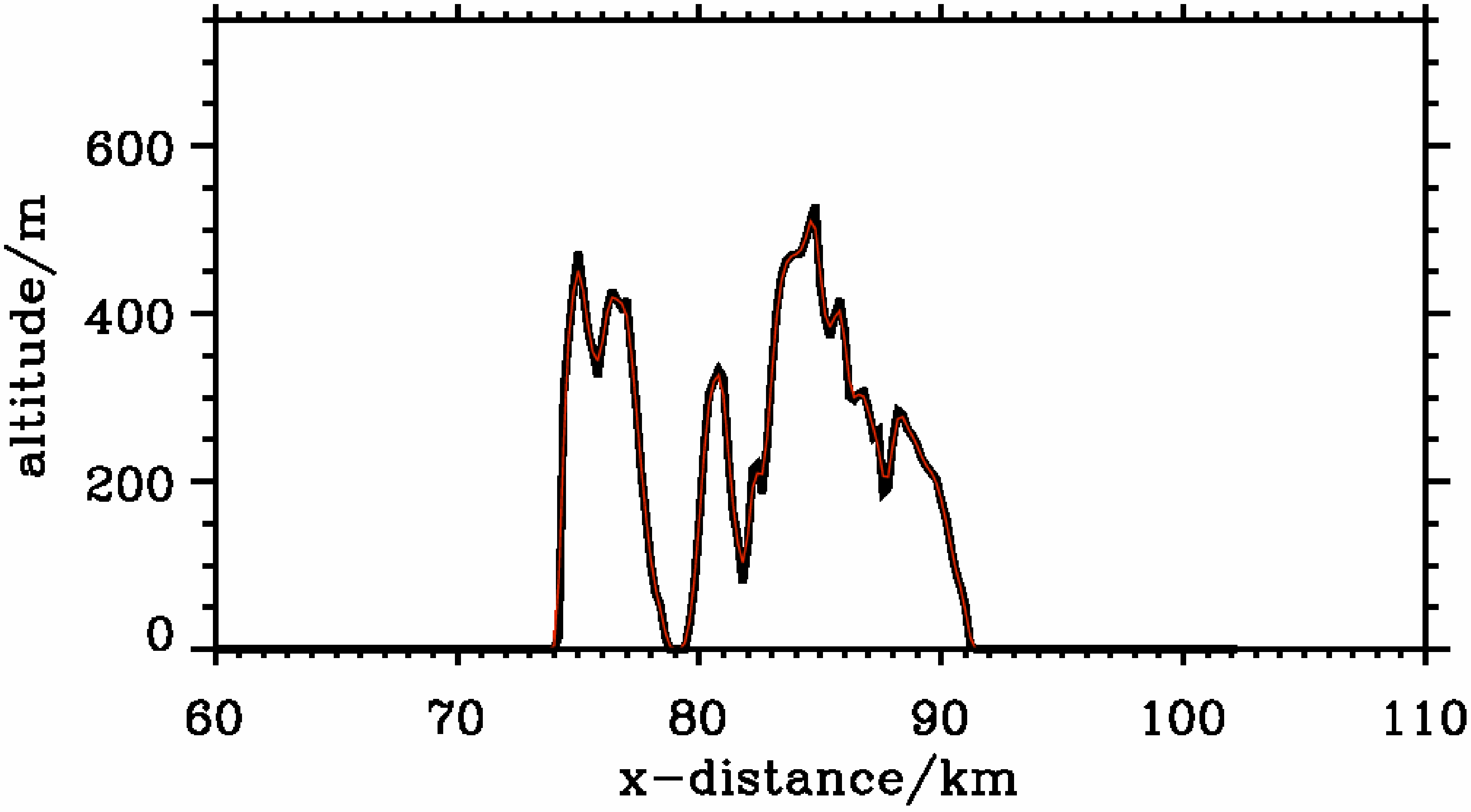

t = 0 min

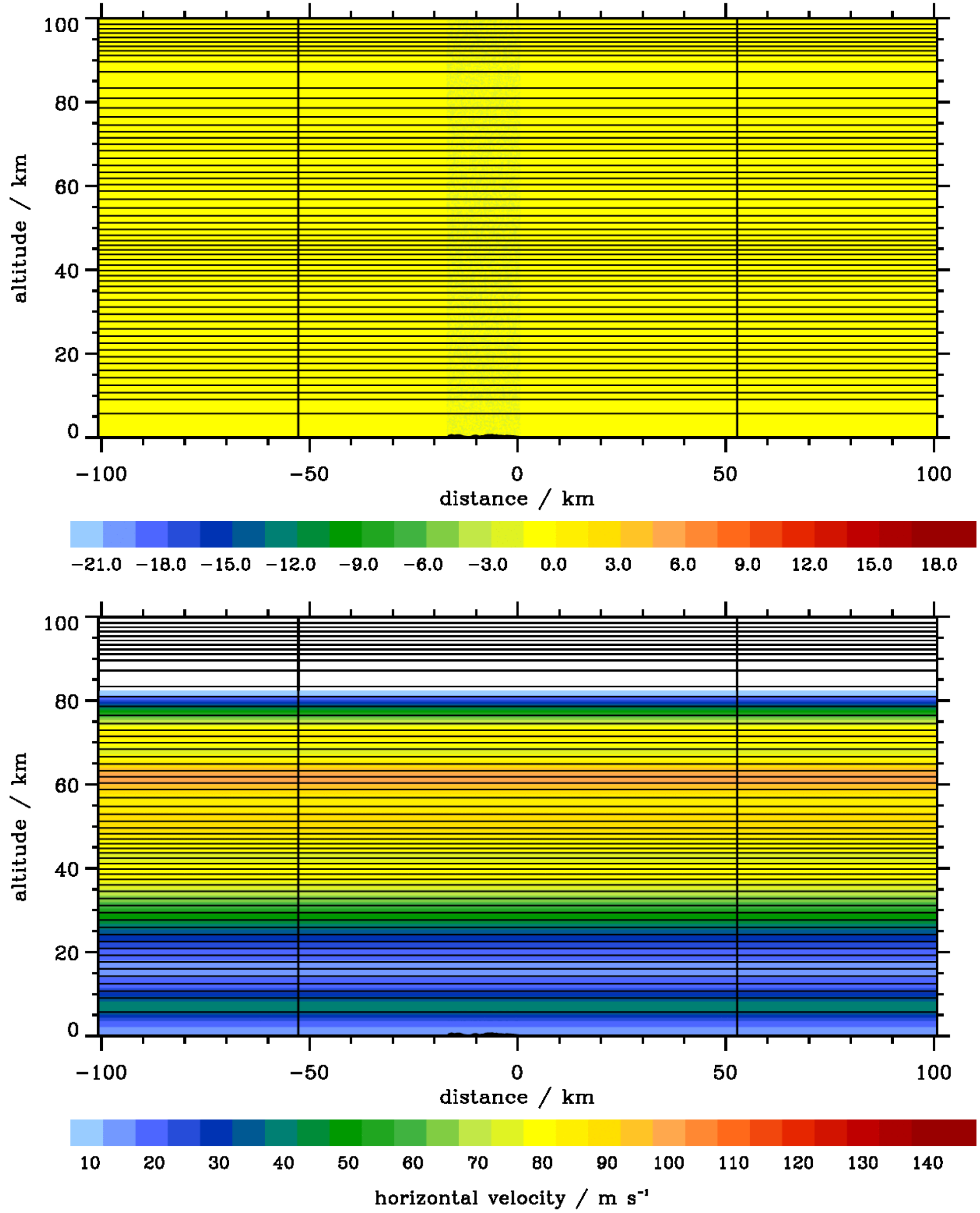

100
80
60
40
20
0
altitude / km
−100
−50
0
50
100
distance / km
−21.0 −18.0 −15.0 −12.0 −9.0 −6.0 −3.0 0.0 3.0 6.0 9.0 12.0 15.0 18.0
altitude / km
distance / km
10 20 30 40 50 60 70 80 90 100 110 120 130 140
horizontal velocity / m s⁻¹

t = 6 min

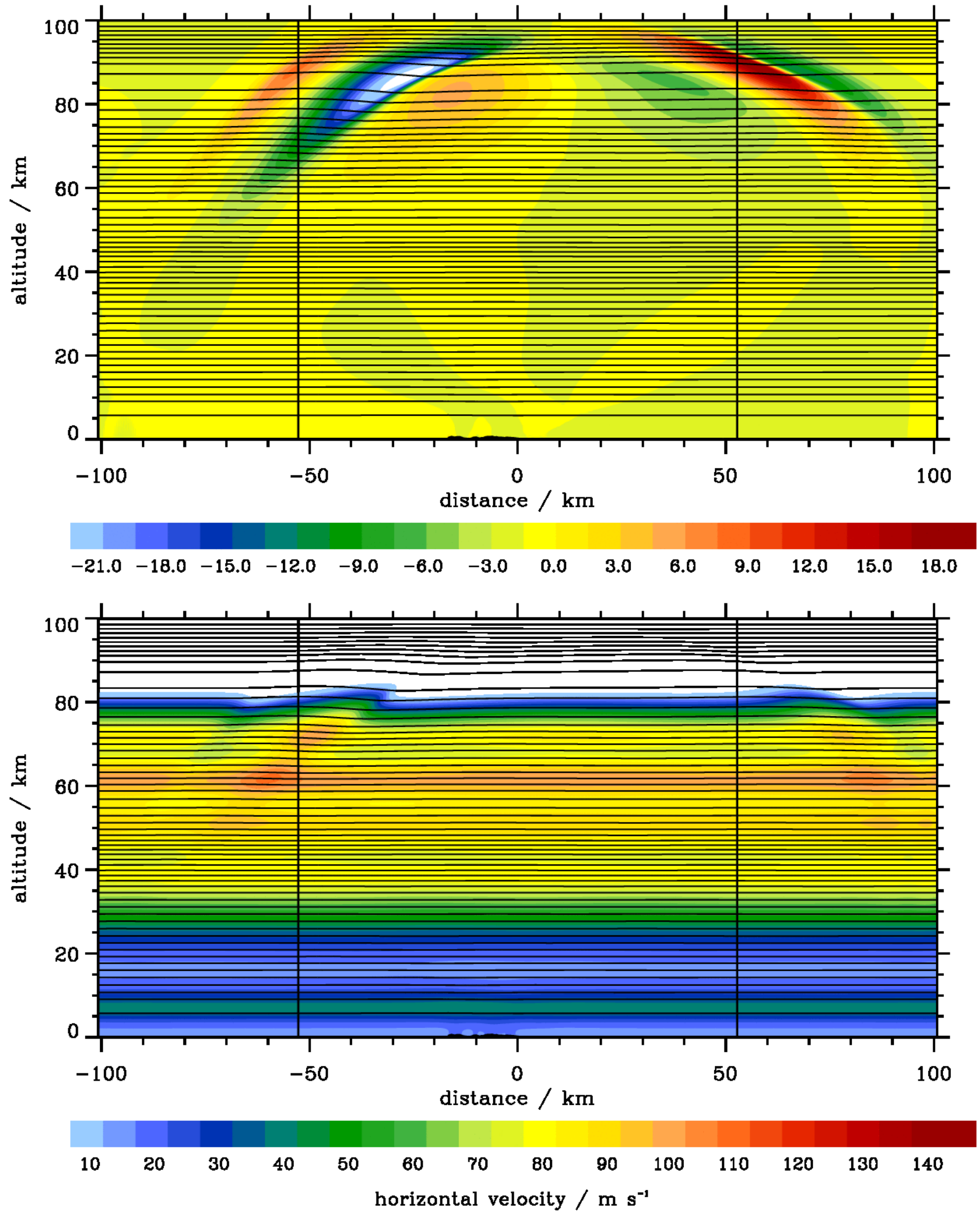

altitude / km
100
80
60
40
20
0
−100
−50
0
50
100
distance / km
−21.0 −18.0 −15.0 −12.0 −9.0 −6.0 −3.0 0.0 3.0 6.0 9.0 12.0 15.0 18.0
altitude / km
distance / km
10 20 30 40 50 60 70 80 90 100 110 120 130 140
horizontal velocity / m s⁻¹

t = 60 min

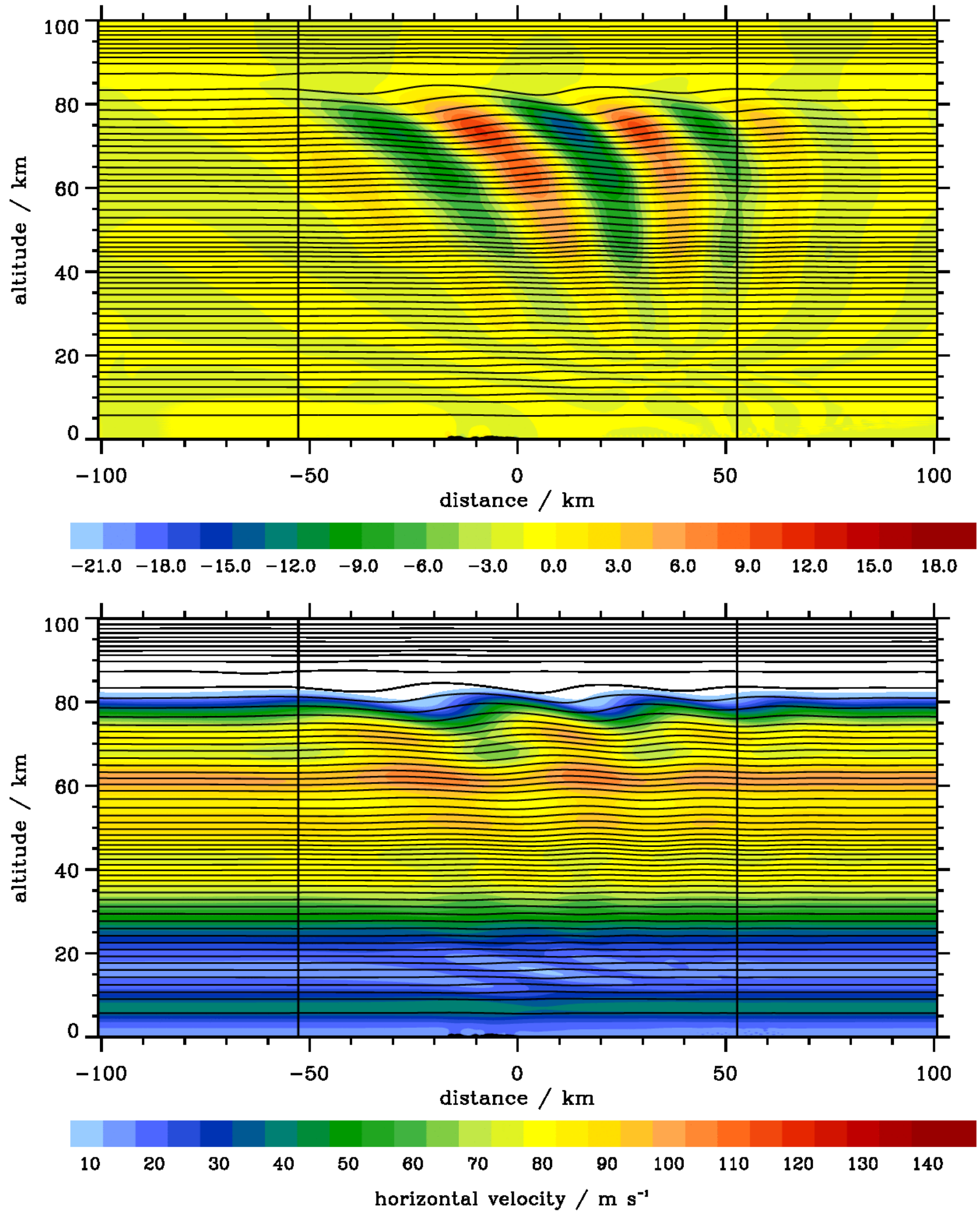

altitude / km
distance / km
−21.0 −18.0 −15.0 −12.0 −9.0 −6.0 −3.0 0.0 3.0 6.0 9.0 12.0 15.0 18.0
altitude / km
distance / km
10 20 30 40 50 60 70 80 90 100 110 120 130 140
horizontal velocity / m s⁻¹

t = 90 min

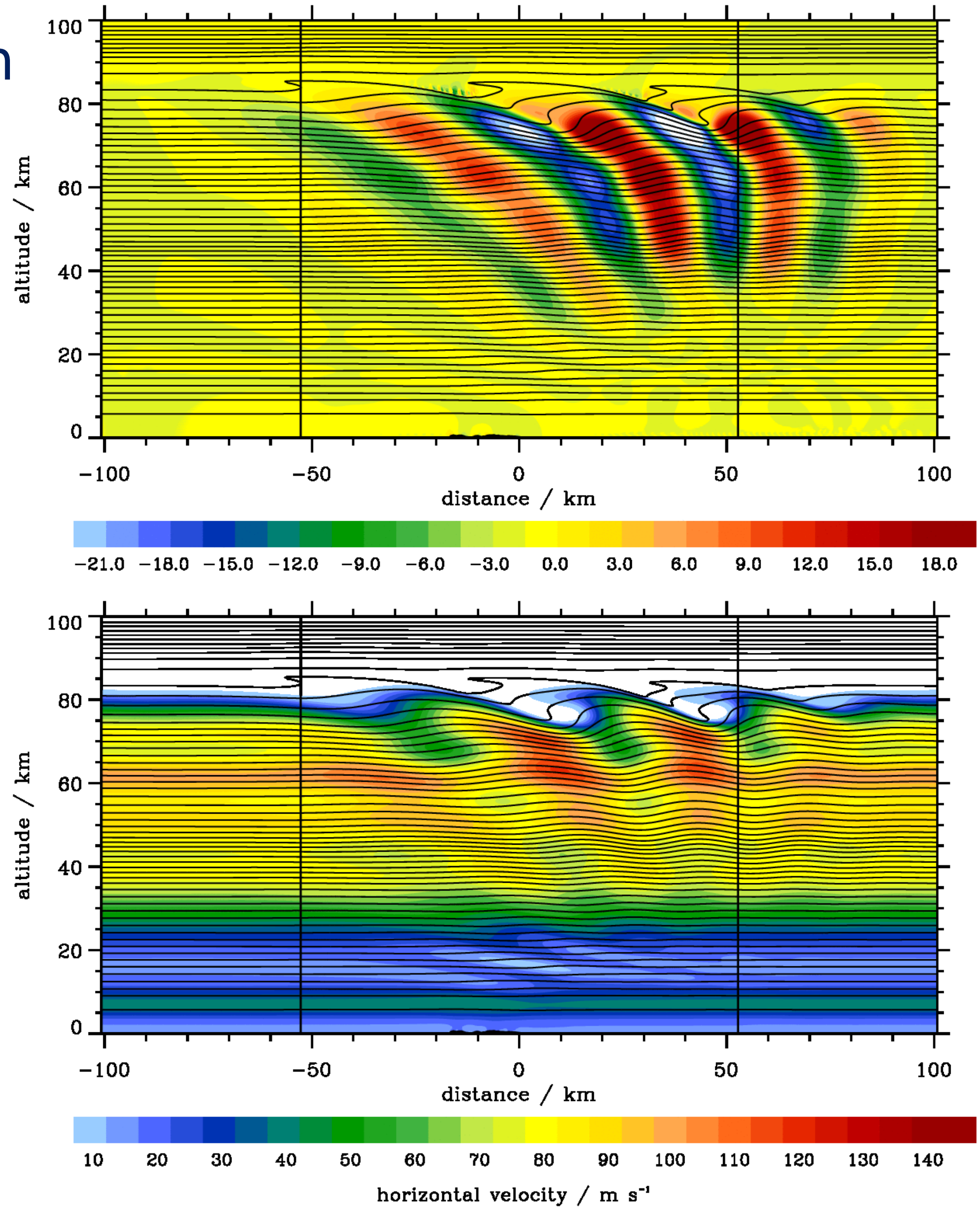

100
80
60
40
20
0
altitude / km
−100
−50
0
50
100
distance / km
−21.0
−18.0
−15.0
−12.0
−9.0
−6.0
−3.0
0.0
3.0
6.0
9.0
12.0
15.0
18.0
100
80
60
40
20
0
altitude / km
−100
−50
0
50
100
distance / km
10
20
30
40
50
60
70
80
90
100
110
120
130
140
horizontal velocity / m s⁻¹

t = 90 min

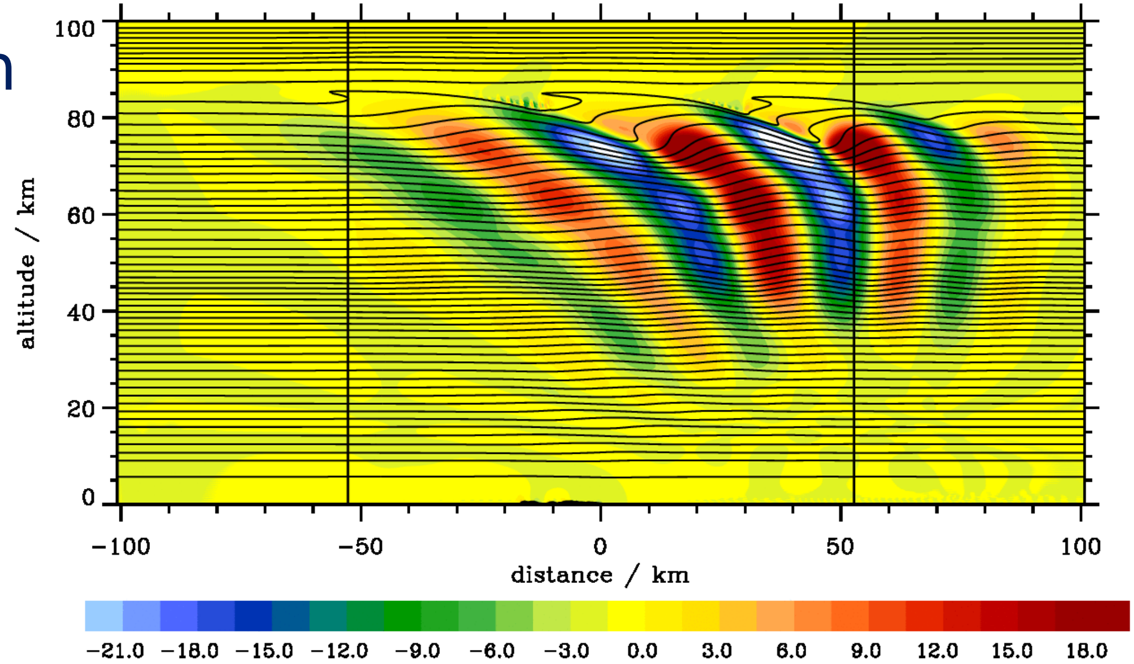

altitude / km
distance / km
100
80
60
40
20
0
−100
−50
0
50
100
−21.0 −18.0 −15.0 −12.0 −9.0 −6.0 −3.0 0.0 3.0 6.0 9.0 12.0 15.0 18.0

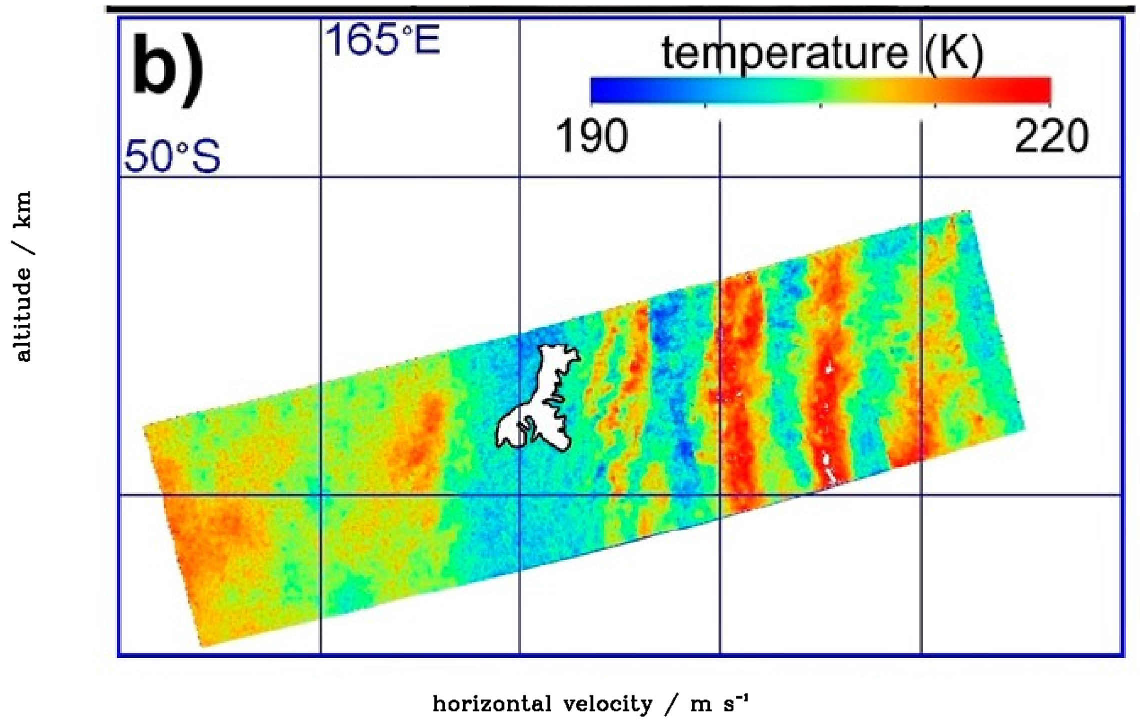

b)
165°E
50°S
temperature (K)
190
220
altitude / km
horizontal velocity / m s⁻¹

t = 120 min

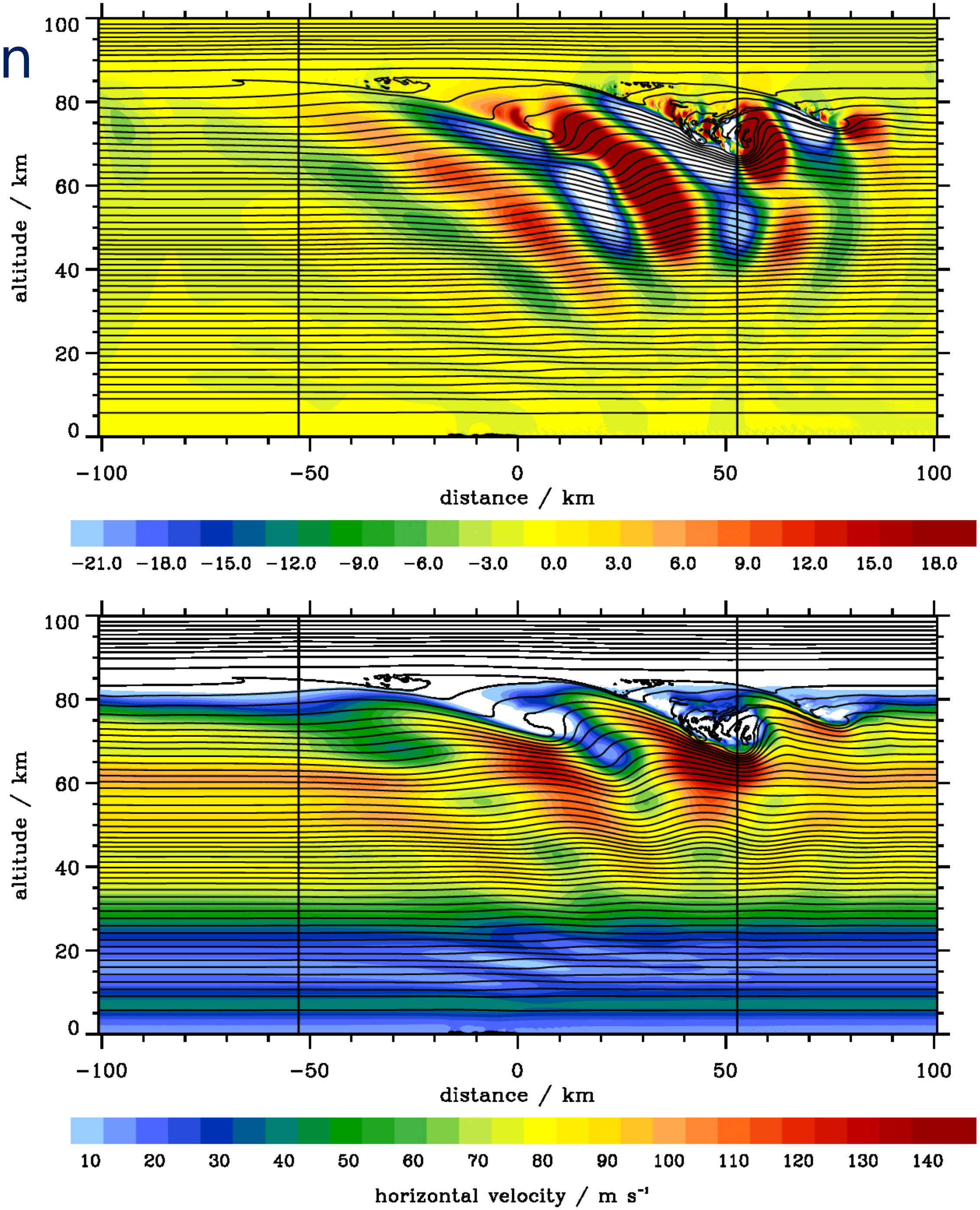

altitude / km
distance / km
−21.0 −18.0 −15.0 −12.0 −9.0 −6.0 −3.0 0.0 3.0 6.0 9.0 12.0 15.0 18.0
altitude / km
distance / km
10 20 30 40 50 60 70 80 90 100 110 120 130 140
horizontal velocity / m s⁻¹

EULAG Simulations for Auckland Case RF23

- good agreement of simulated horizontal wavelength with observed wavelength and solutions from Fourier Ray Modelling – until breaking sets in: really dominant linear dynamics

- breaking happens in gigantic rolls which sit like rotors on the underlying waves – **mesospheric rotors**:
  - steep, deeply penetrating nonhydrostatic gravity waves act like elevated, quasi-stationary mountains producing „downslope wind storms“
  - generate broad warm anomalies (Foehn, Chinook) and narrow cold anomalies like fronts (hydraulic jumps); see Mike‘s talk yesterday

- inviscid 2D simulations certainly overestimate w and T‘ but the code is very robust to simulate the deep dynamics properly

- strong dependency of upper air dynamics (z > 60 km) on initial and background profiles

Mesospheric Rotors

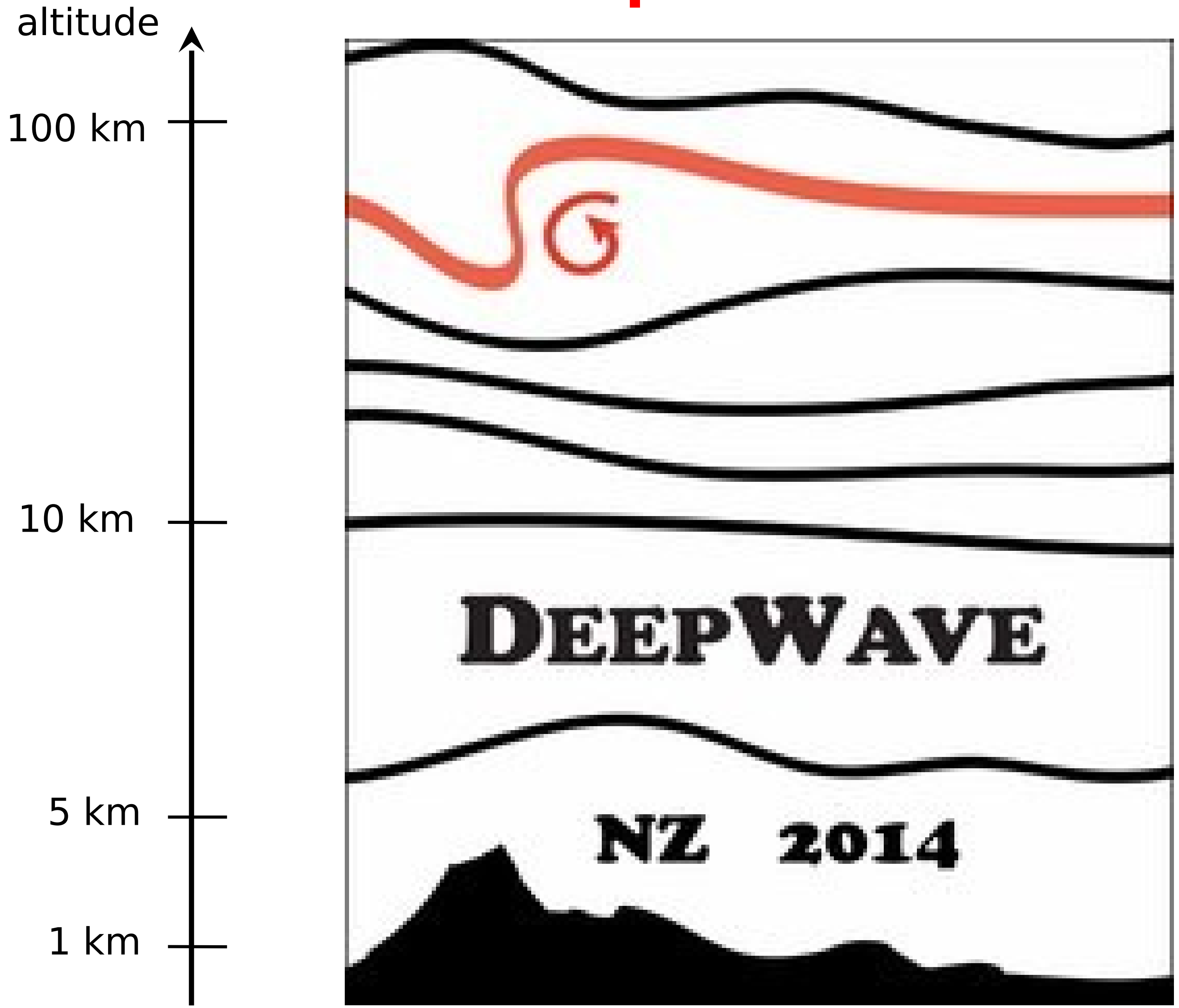

RF05 16 June 2014

- why RF05??

(1) Smith & Kruse (2017) show observed broad spectra but no simulations – „… one of the most rugged terrains in the world. Small-scale relief exceeds 1 km in the high mountain areas (Korup et al. 2005). This roughness broadens the terrain spectrum and the associated wave spectra found in the atmosphere."

Is the rougged terrain alone responsible for the broad spectra? Are these short waves observational artifacts? Do we understand their origins?

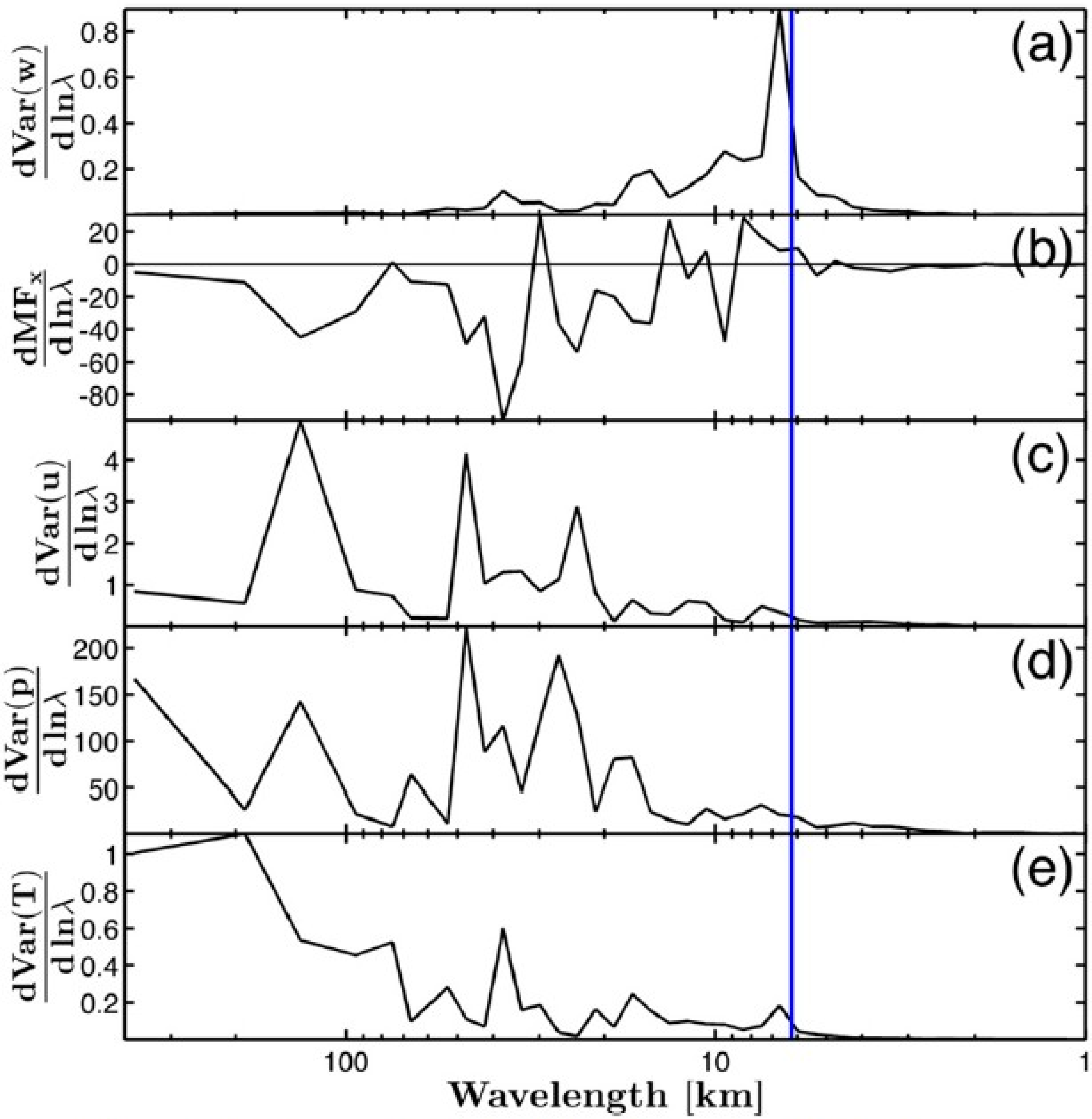

FIG. 9. Aircraft-derived spectra for Mt. Cook flight RF05, leg 11 on 16 Jun 2014: (a) w power, (b) MFx, (c) u power, (d) p power, and (e) T power. The vertical blue line is the estimated buoyancy cutoff for this leg. Note the shift in dominant wavelength between (a) and (c)–(e).

RF05 16 June 2014

- why RF05??

(2) GV-Summary (by Ron): „ …The pattern of waves across the island was very repeatable leg after leg. Near 170E, the UIC drops from about 20m/s to 10m/s, slight turbulence is found and short wave train begins. Typical amplitude of the vertical velocity in the wave train was 2 m/s. The wavelength was about 10km. It extends usually all the way to the east end of the leg. It is the longest wave oscillation I have ever seen on the atmosphere with about 30 full oscillations. Over the ridge crest, there were longer non-periodic waves that were probably vertically propagating. …”

Comparison to observations and other models

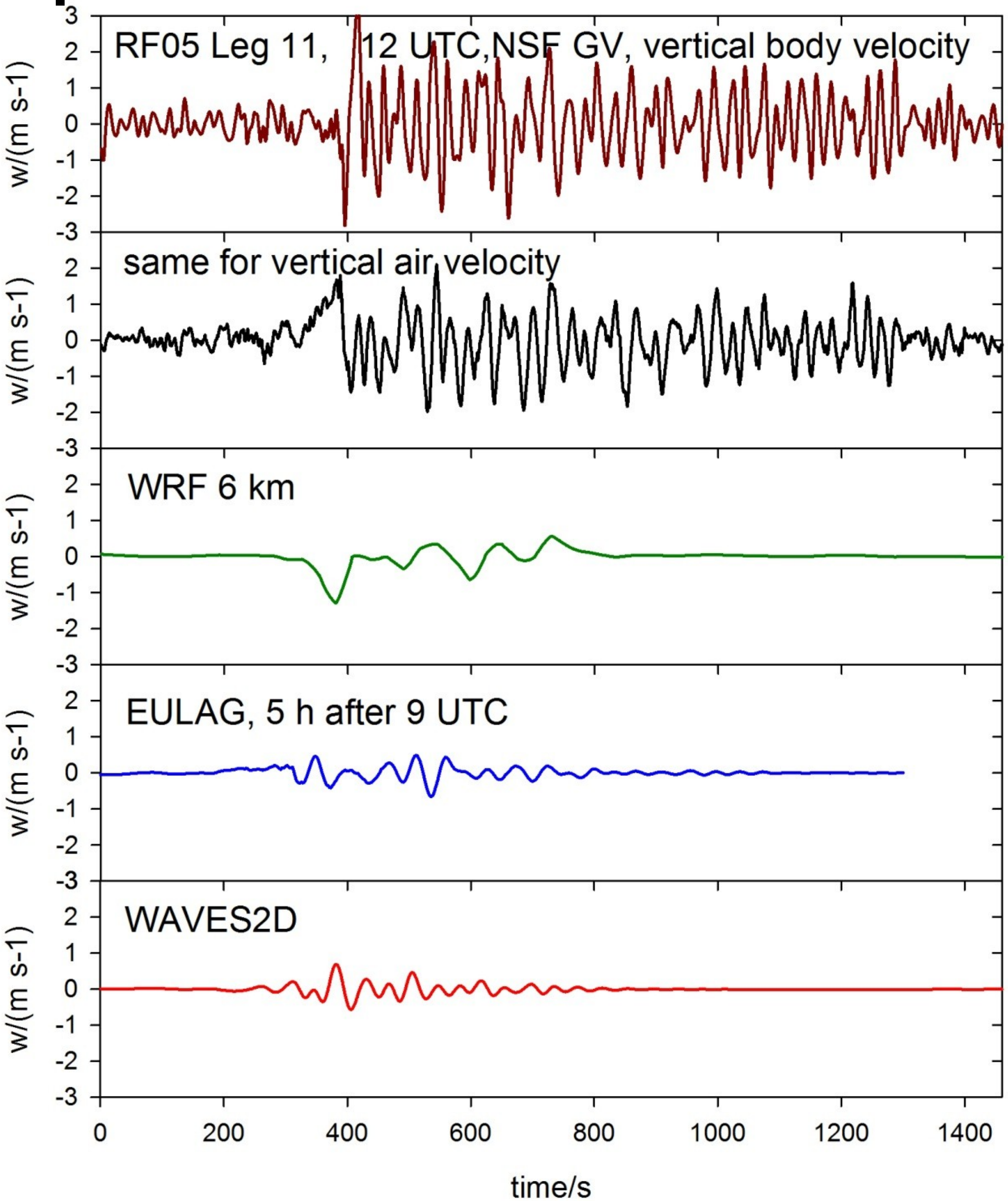

NCAR: VSPD

NCAR: WIP

Chris Kruse

Andreas Dörnbrack, preliminary

Ulrich Schumann (presentation given 20 July at DLR, see next talk)

EULAG Simulations

- initial/background profiles: ECMWF <u>upstream</u> profiles 06, 07, …., 13 UTC
- inviscid, compressible runs
- dx=500 m, dz=200 m, dt=0.5 s
- simulation time 12 h
- smooth and rough topographies of Mt Cook 1b
- ongoing: sensitivity studies (absorber, Rayleigh damping time scale, resolution, set of equations, vertical coordinate transformations, …)

ECMWF IFS Upstream Profiles 16 June 2016 12 UTC

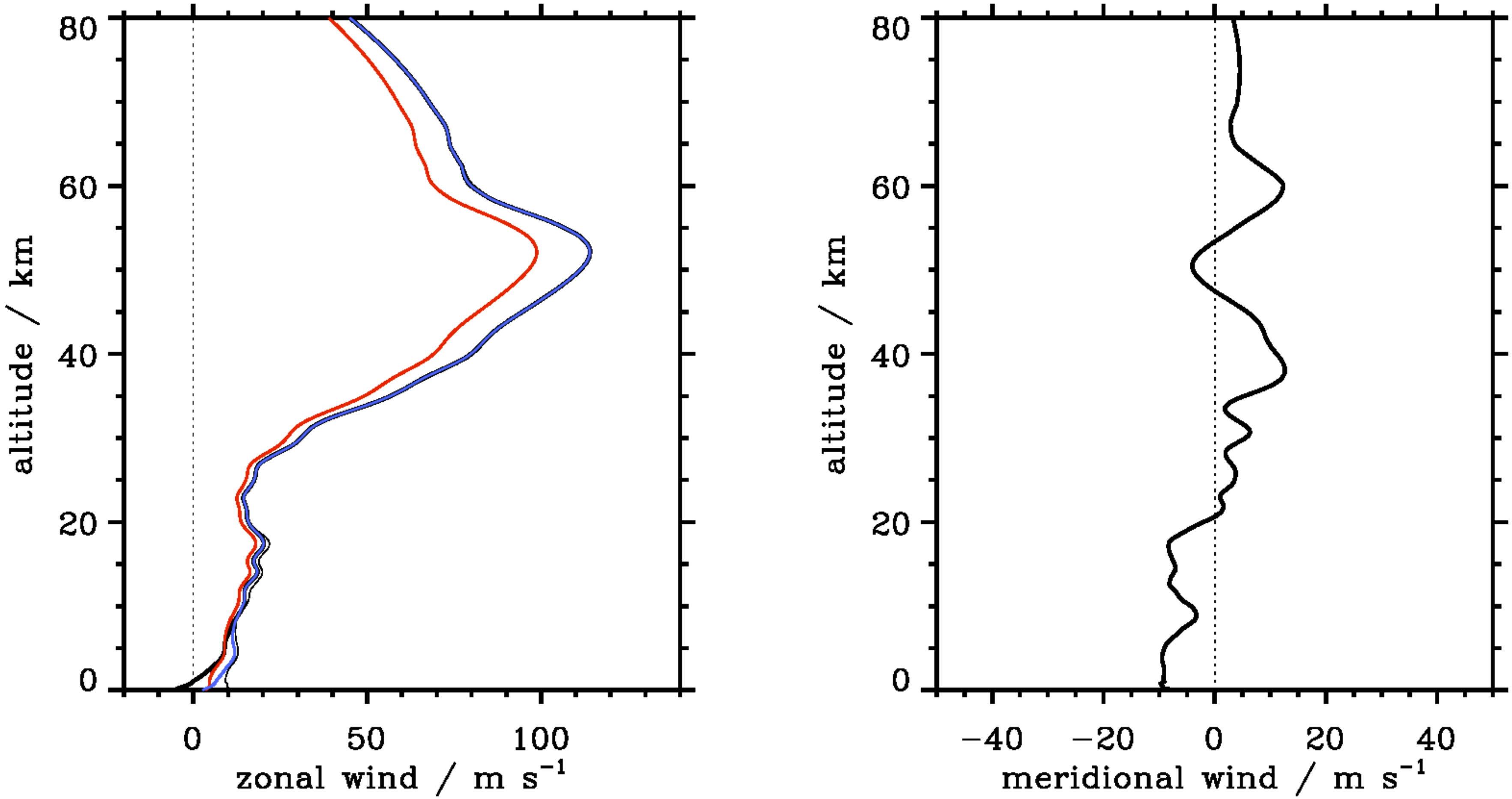

thick black line: u **red line**: u_{ROT1} (magnitude of positive $u_{\parallel}$ and $v_{\parallel}$ with 300° along track direction

thin black line: v_H **blue line**: u_{ROT2} (wind direction turns from 320° to 270° in the lowest 10 km)

ECMWF IFS Upstream Profiles 16 June 2016 12 UTC

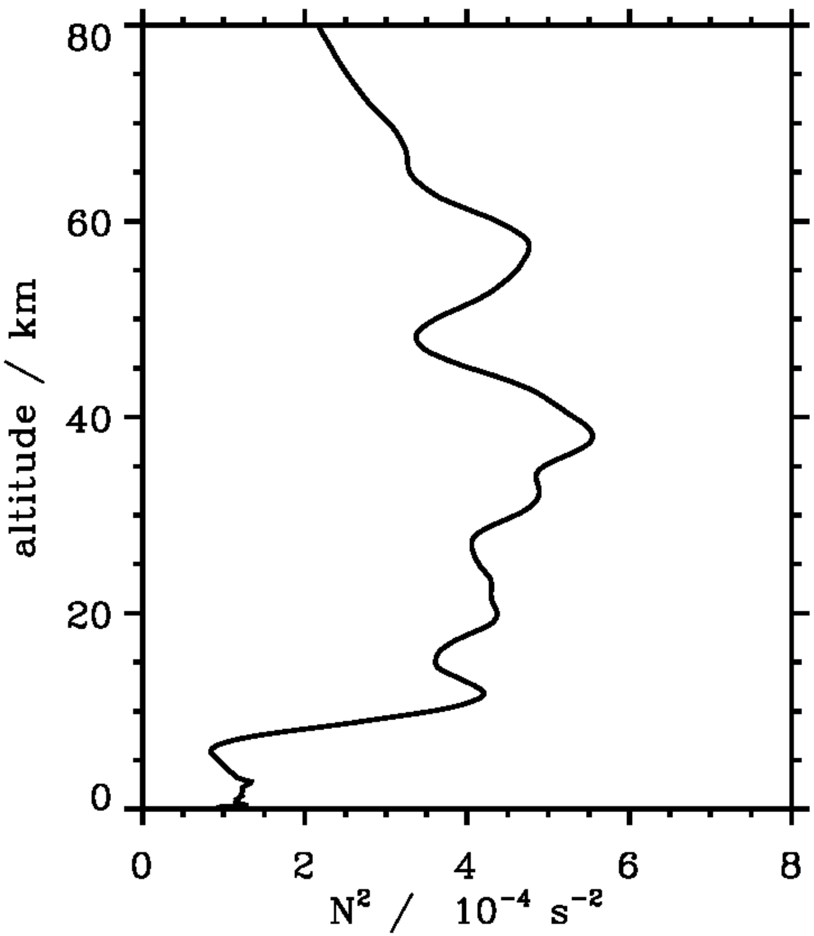

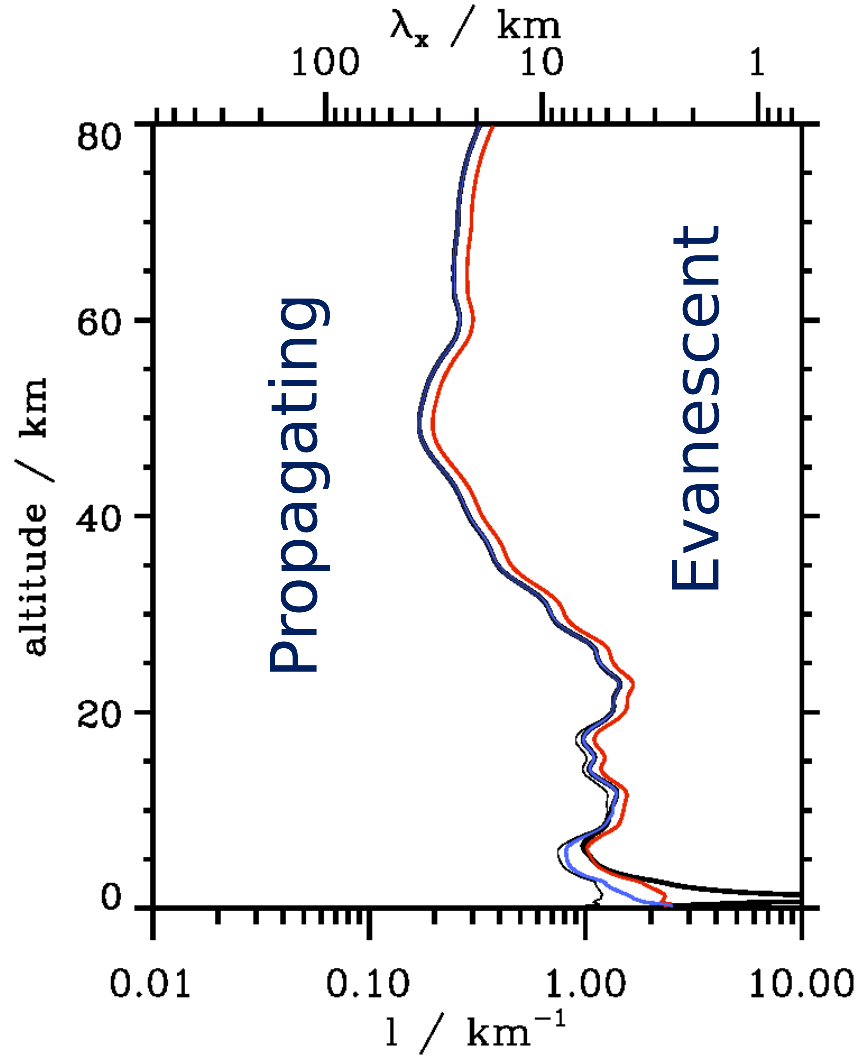

thick black line: u **red line**: u_{ROT1} (magnitude of positive $u_\parallel$ and $v_\parallel$ with 300° along track direction

thin black line: v_H **blue line**: u_{ROT2} (wind direction turns from 320° to 270° in the lowest 10 km)

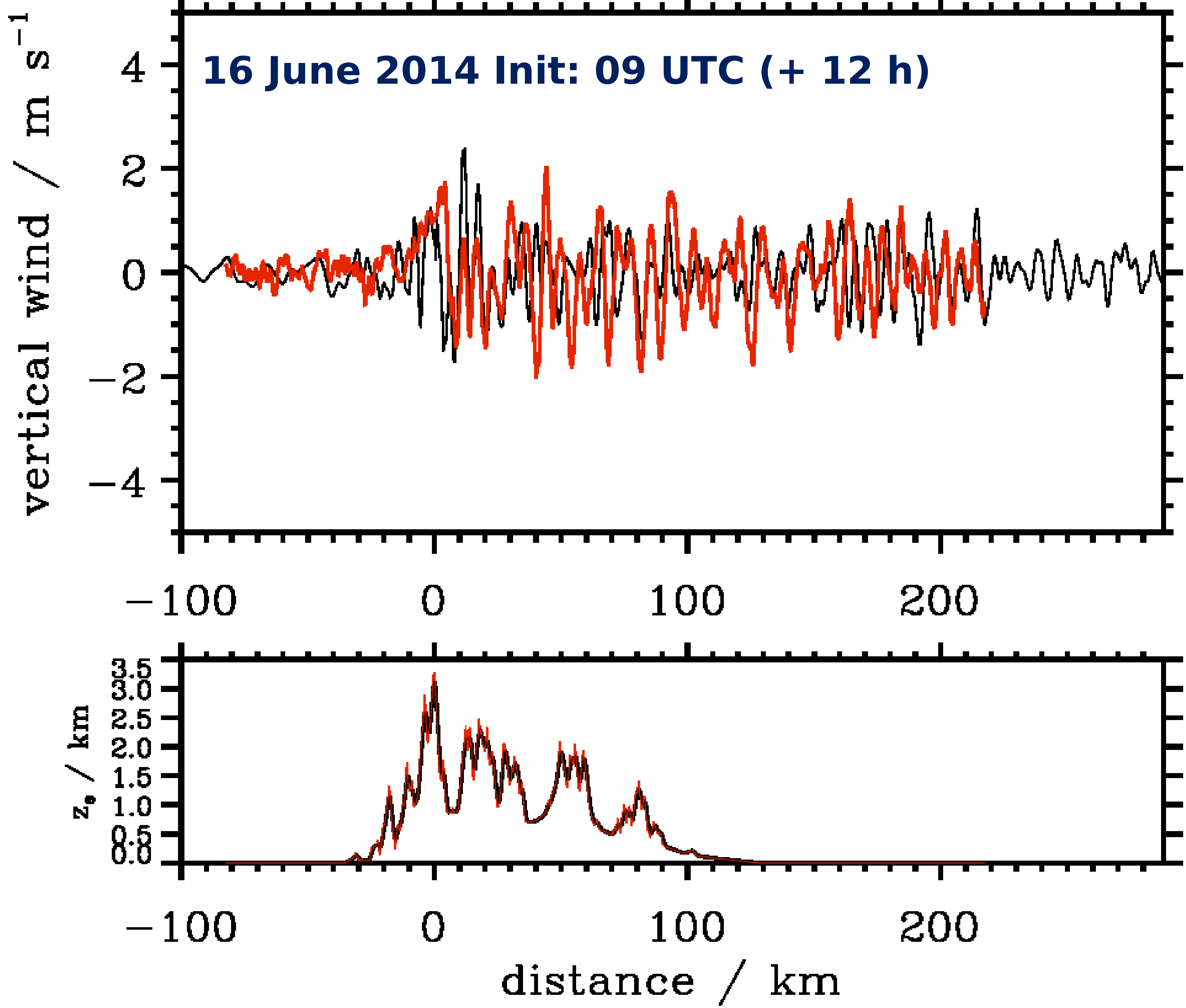

16 June 2014 Init: 09 UTC (+ 12 h)
vertical wind / m s^{-1}
4
2
0
−2
−4
−100
0
100
200
z_s / km
3.5
3.0
2.5
2.0
1.5
1.0
0.5
0.0
−100
0
100
200
distance / km

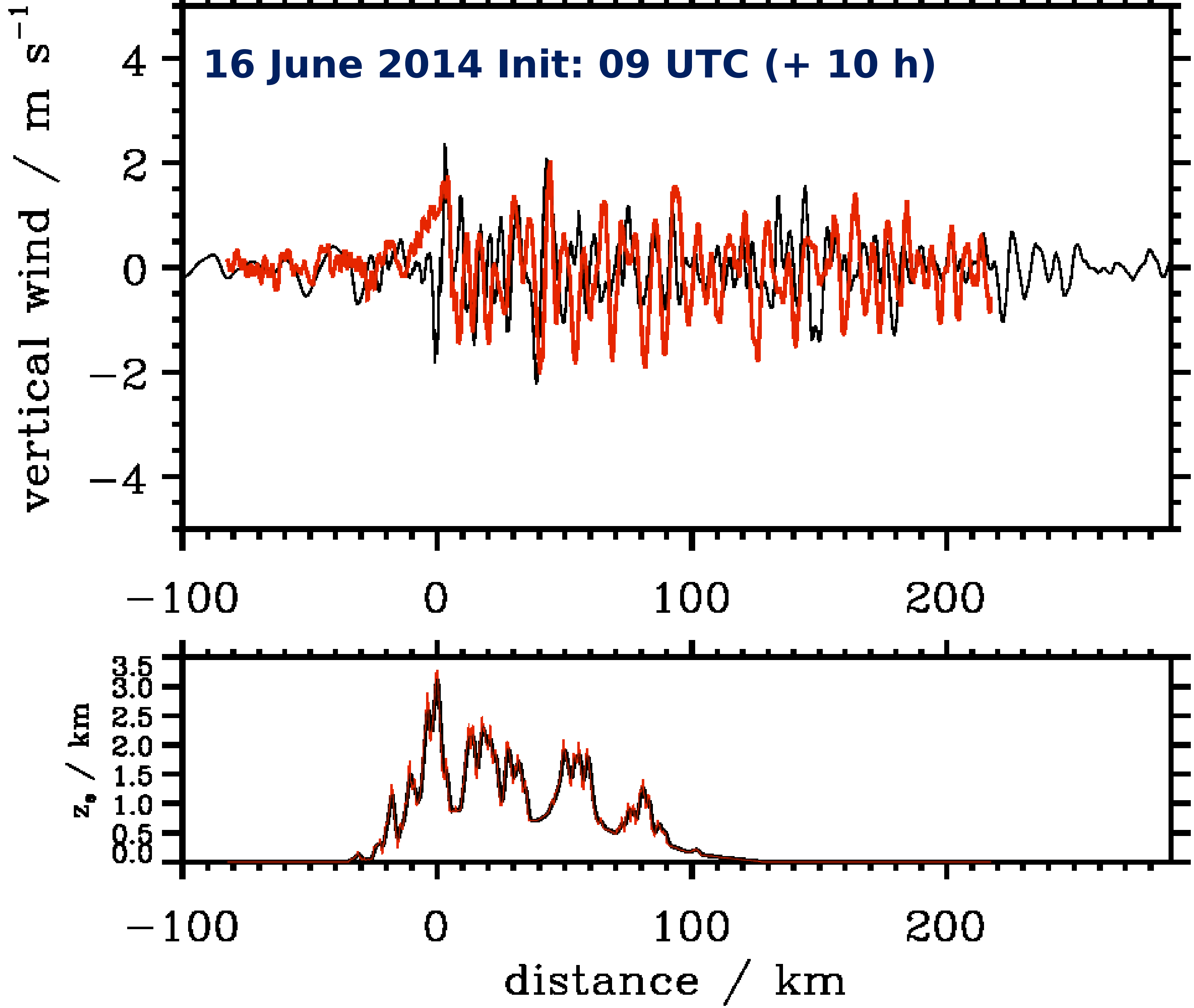
16 June 2014 Init: 09 UTC (+ 10 h)
vertical wind / m s^{-1}
4
2
0
−2
−4
−100
0
100
200
z_s / km
3.5
3.0
2.5
2.0
1.5
1.0
0.5
0.0
−100
0
100
200
distance / km

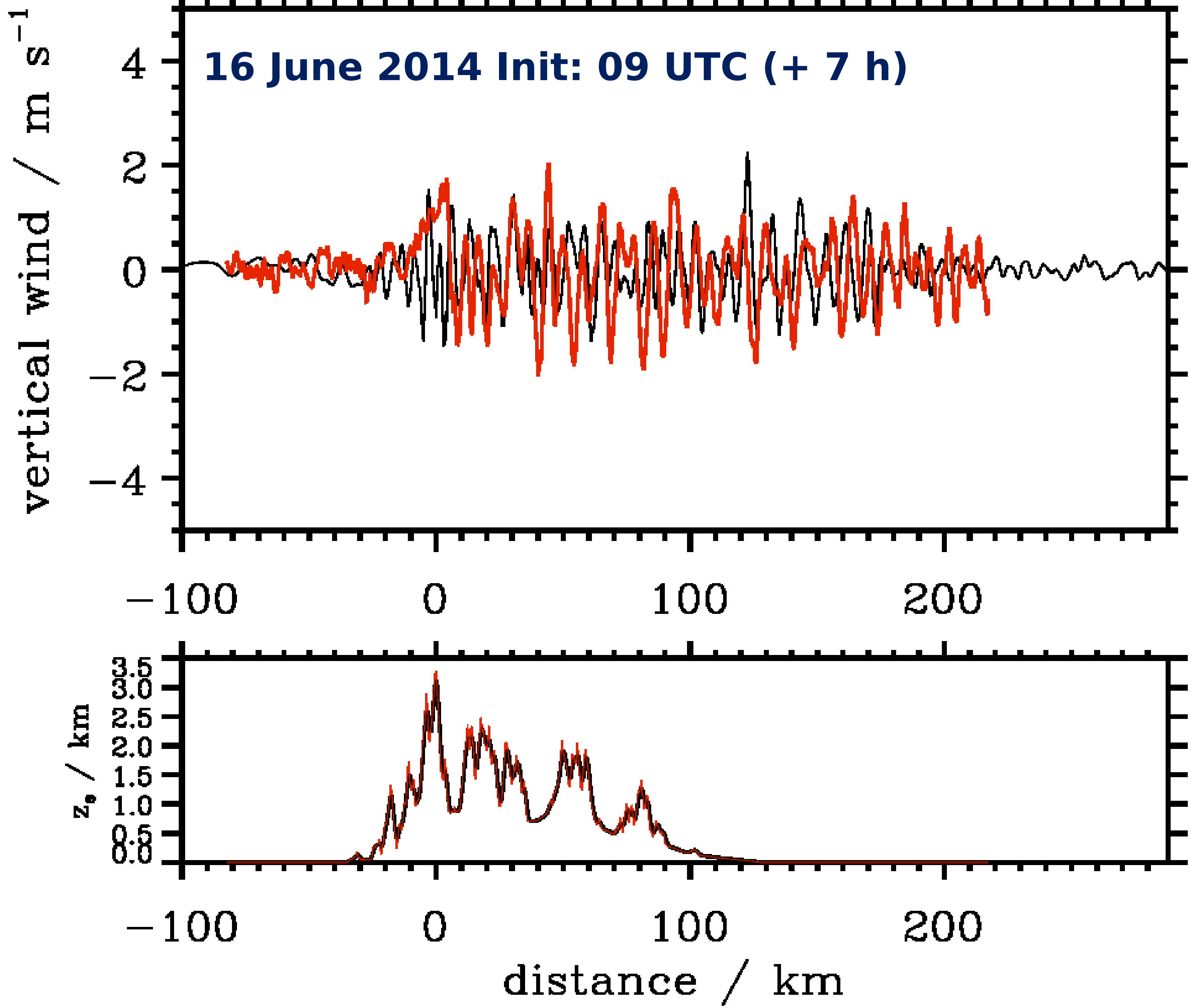

16 June 2014 Init: 09 UTC (+ 7 h)
vertical wind / m s^{-1}
4
2
0
−2
−4
−100
0
100
200
z_s / km
3.5
3.0
2.5
2.0
1.5
1.0
0.5
0.0
−100
0
100
200
distance / km

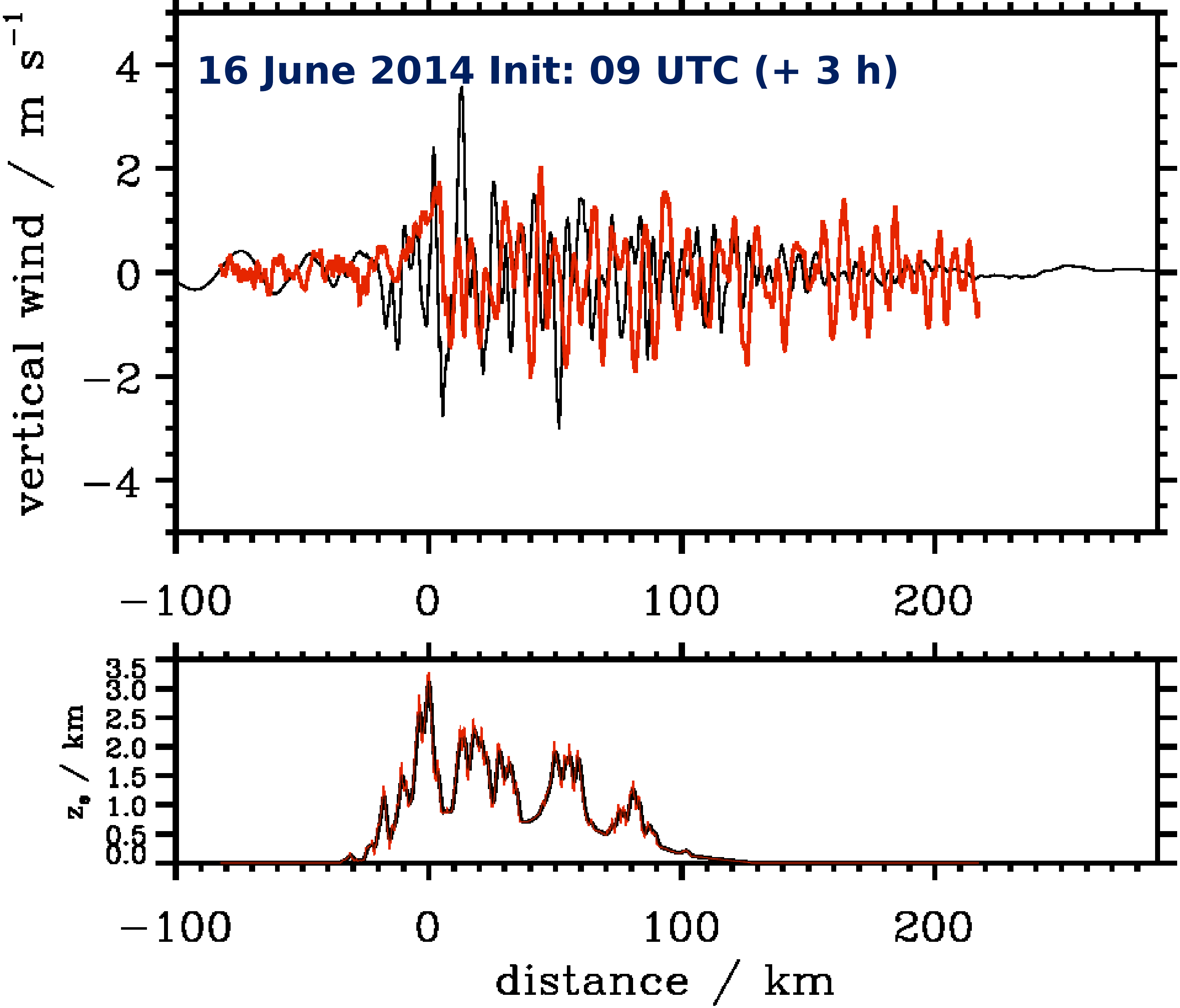
16 June 2014 Init: 09 UTC (+ 3 h)
vertical wind / m s^{-1}
4
2
0
−2
−4
−100
0
100
200
3.5
3.0
2.5
2.0
1.5
1.0
0.5
0.0
z_s / km
−100
0
100
200
distance / km

EULAG u-field every 360 s for 12 h
started at 16 June 2016 12 UTC

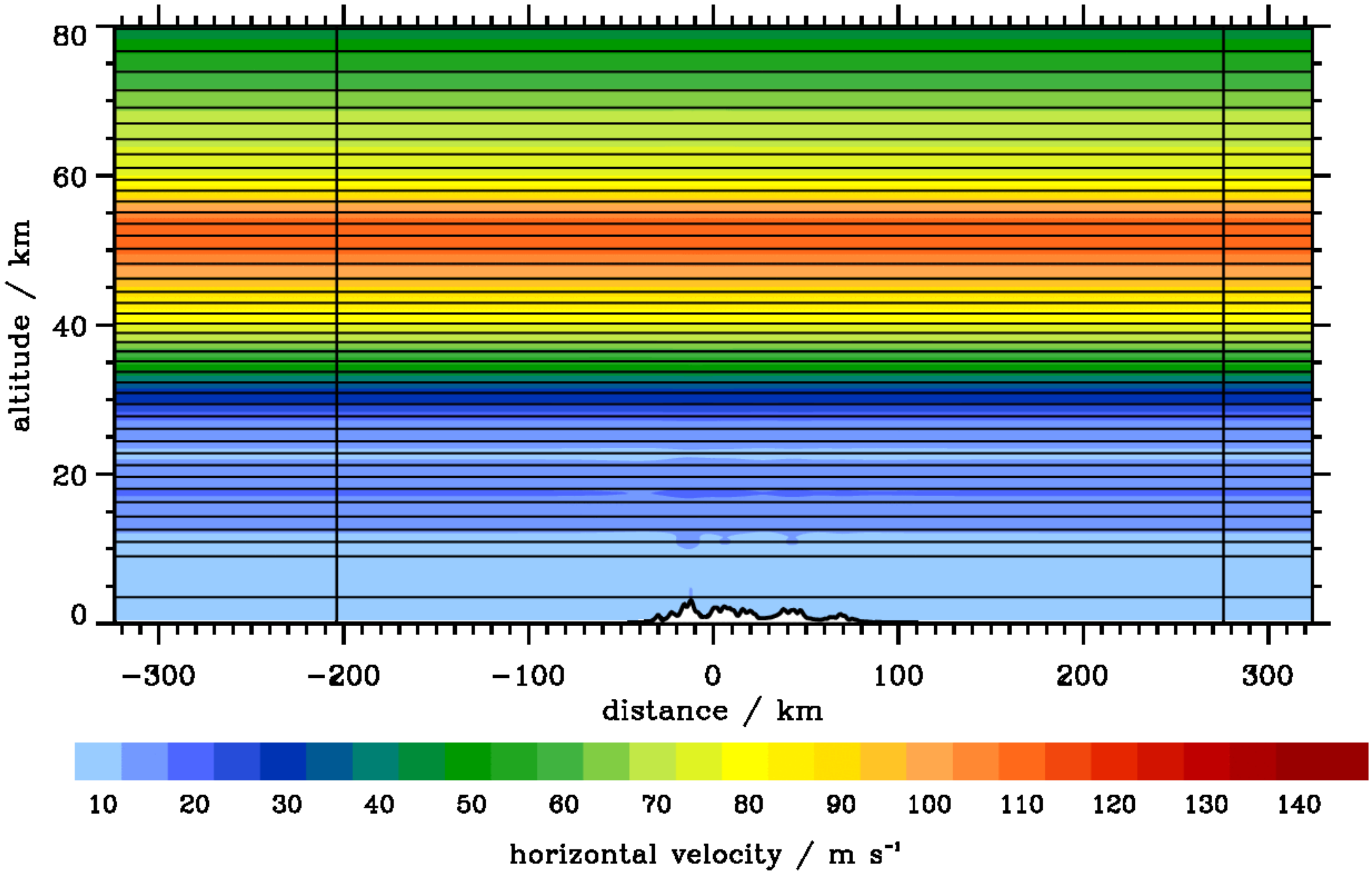

EULAG u-field every 360 s for 12 h started at 16 June 2016 12 UTC

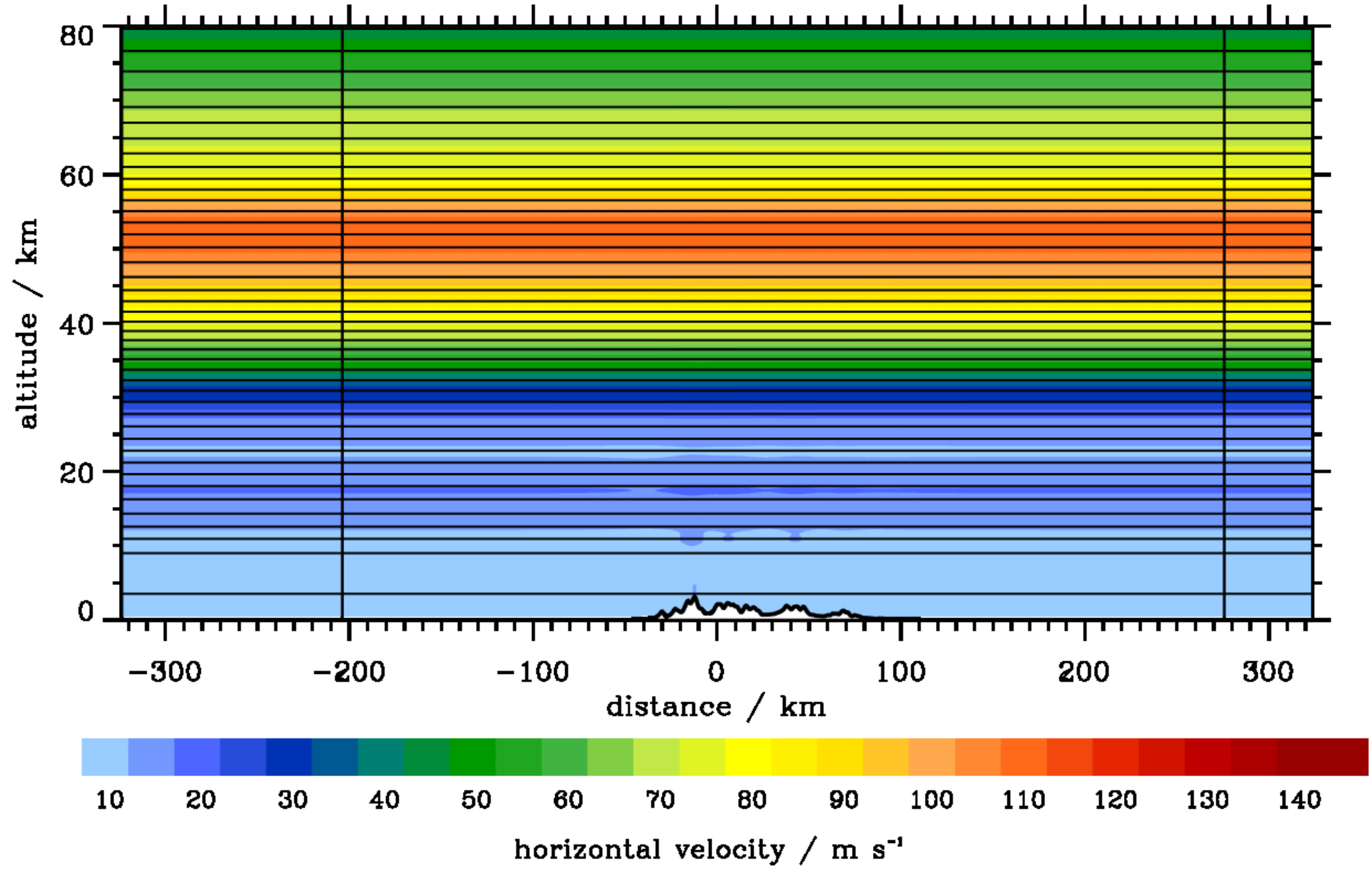

EULAG u-field every 360 s for 12 h started at 16 June 2016 12 UTC

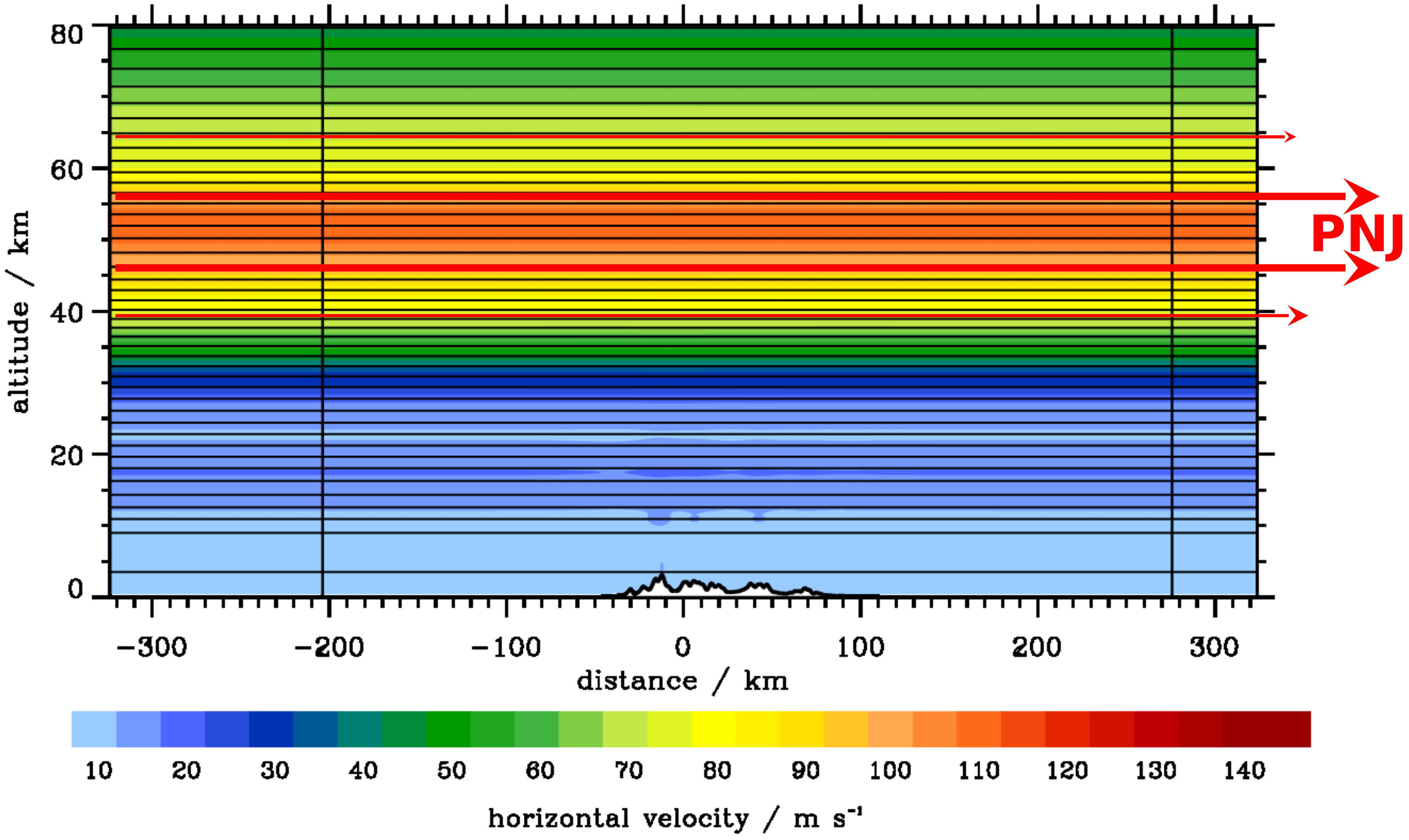

EULAG w-field every 360 s for 12 h started at 16 June 2016 12 UTC

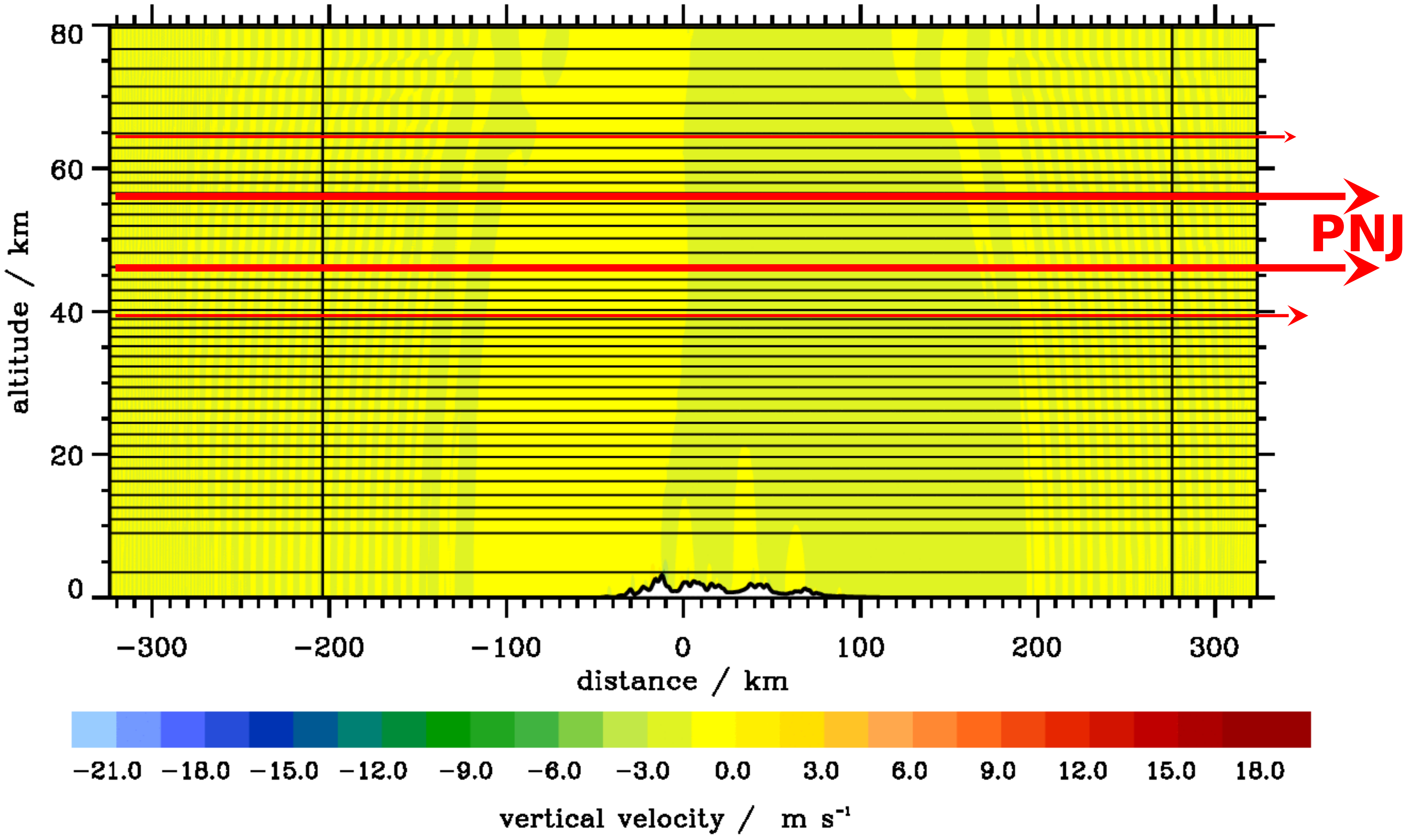

t = 60 min – linear phase of wave propagation

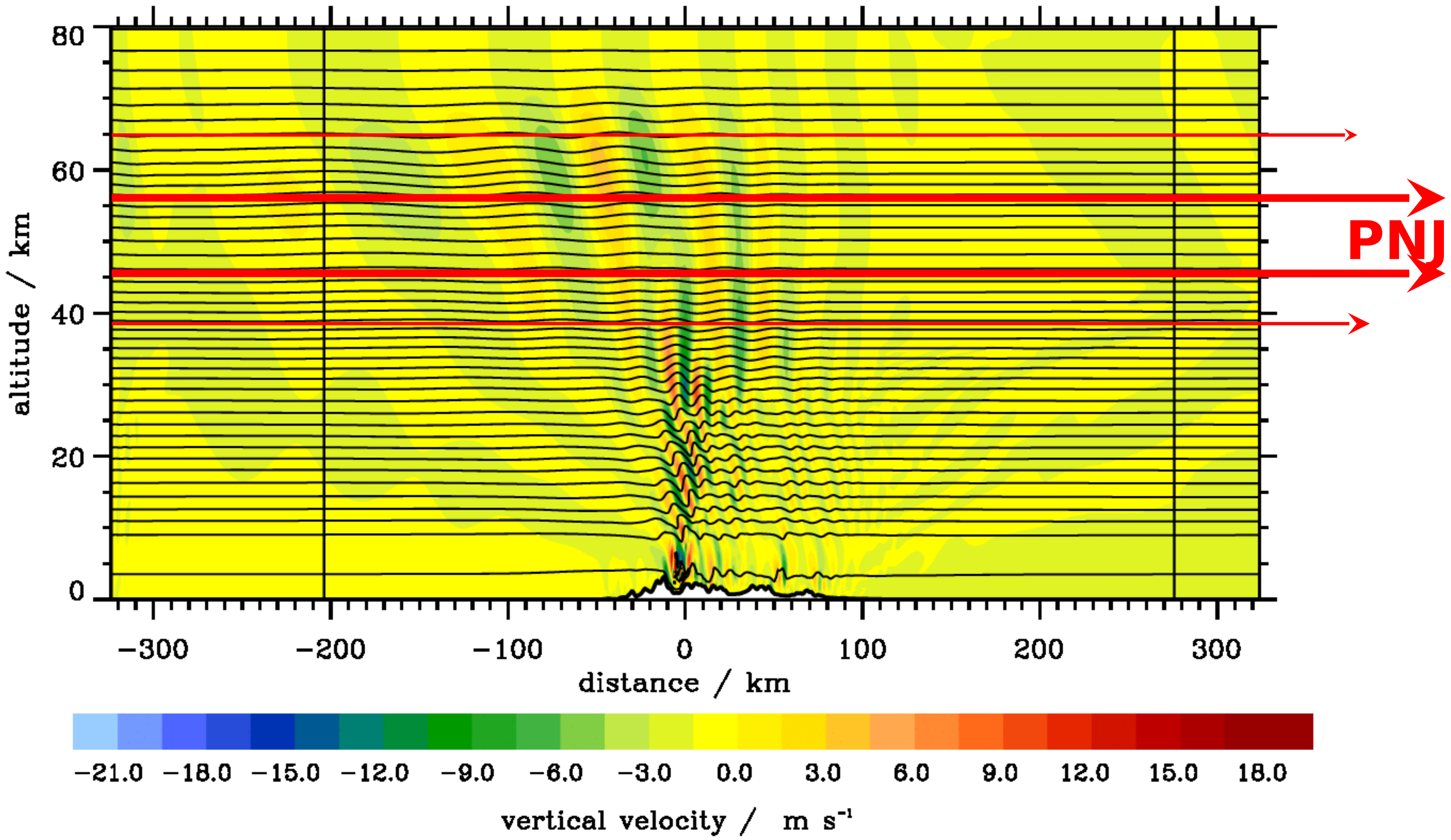

t = 90 min – excitation of stratospheric wave trains

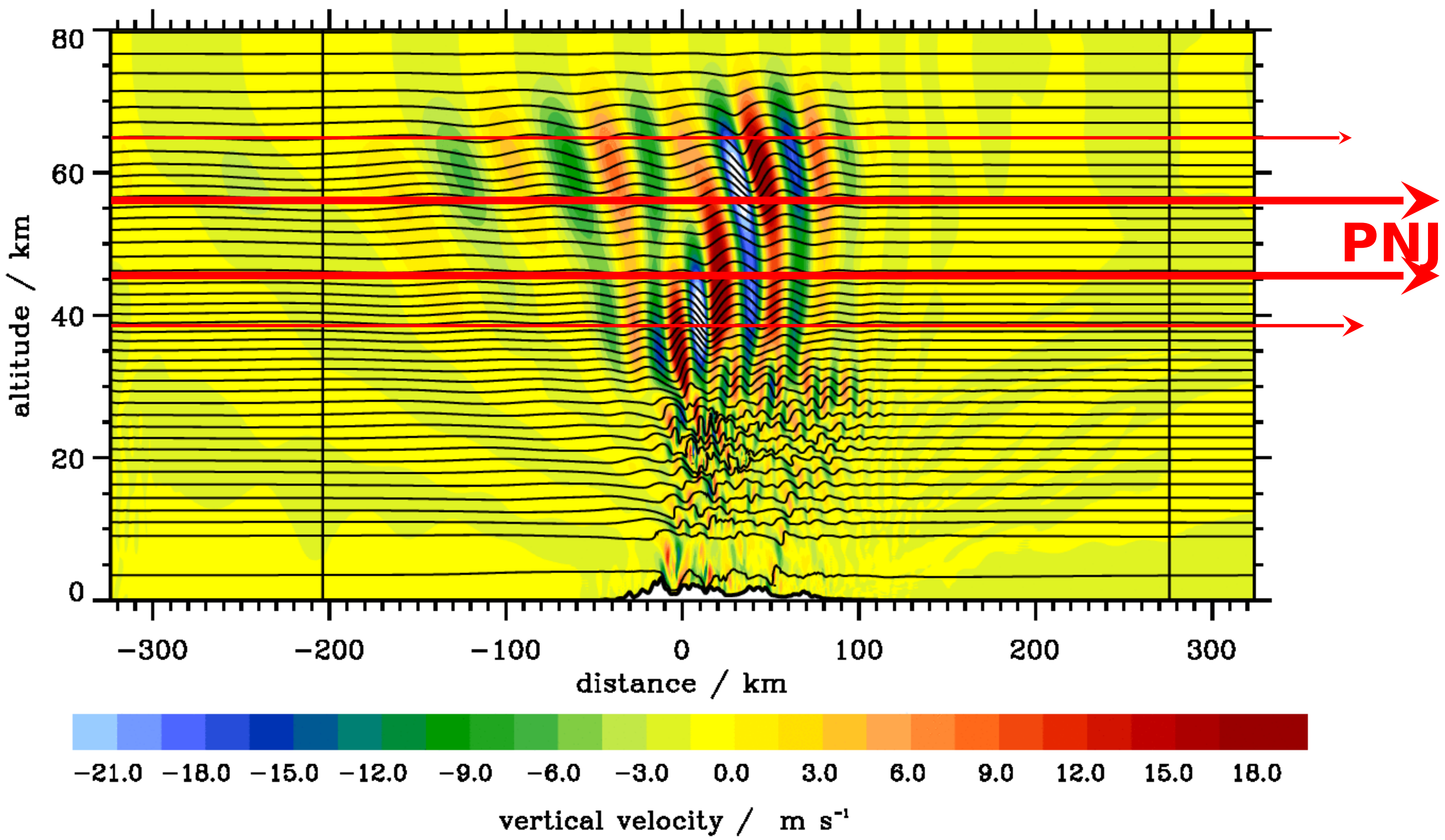

t = 90 min – excitation of stratospheric wave trains

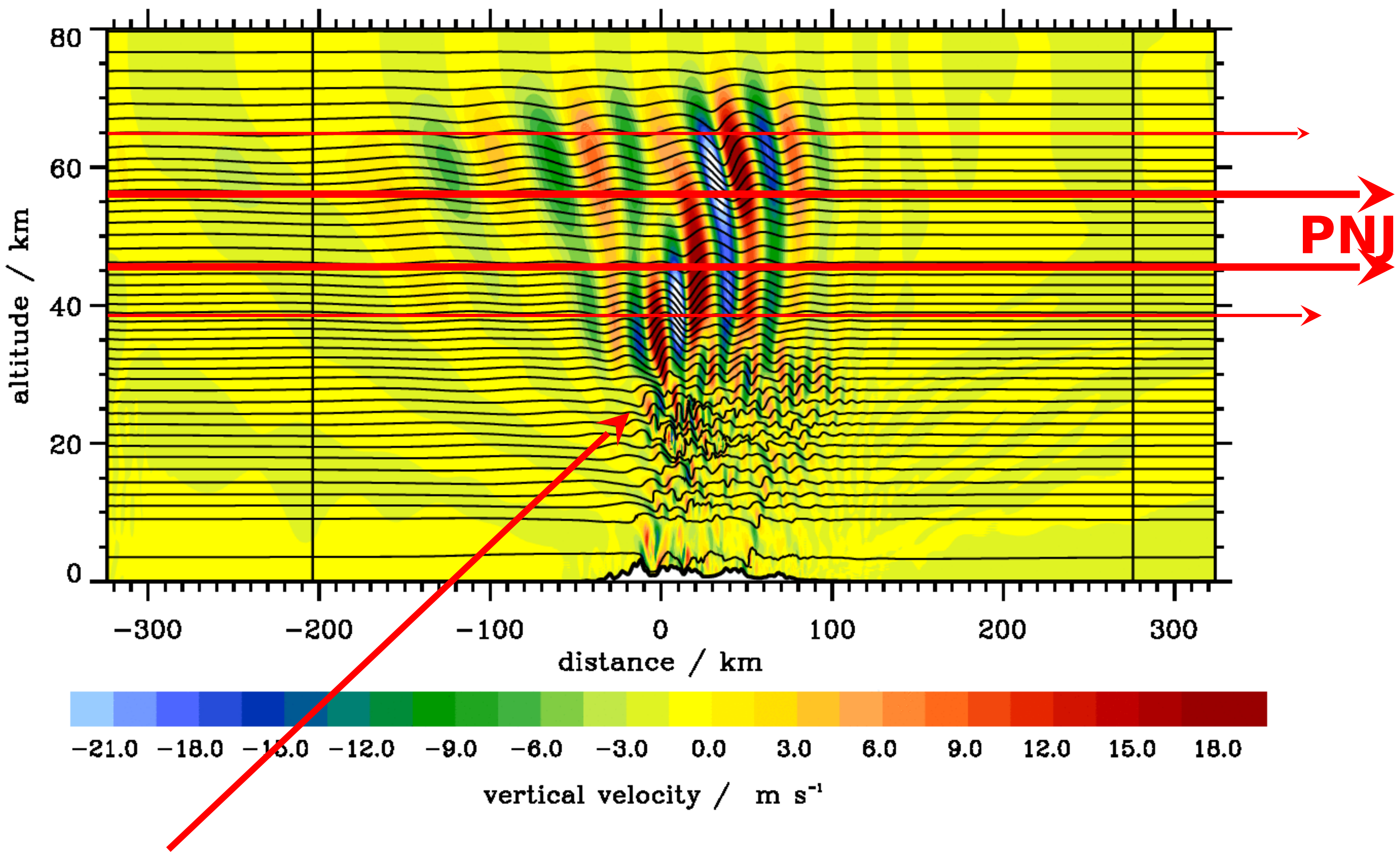

t = 90 min – excitation of stratospheric wave trains

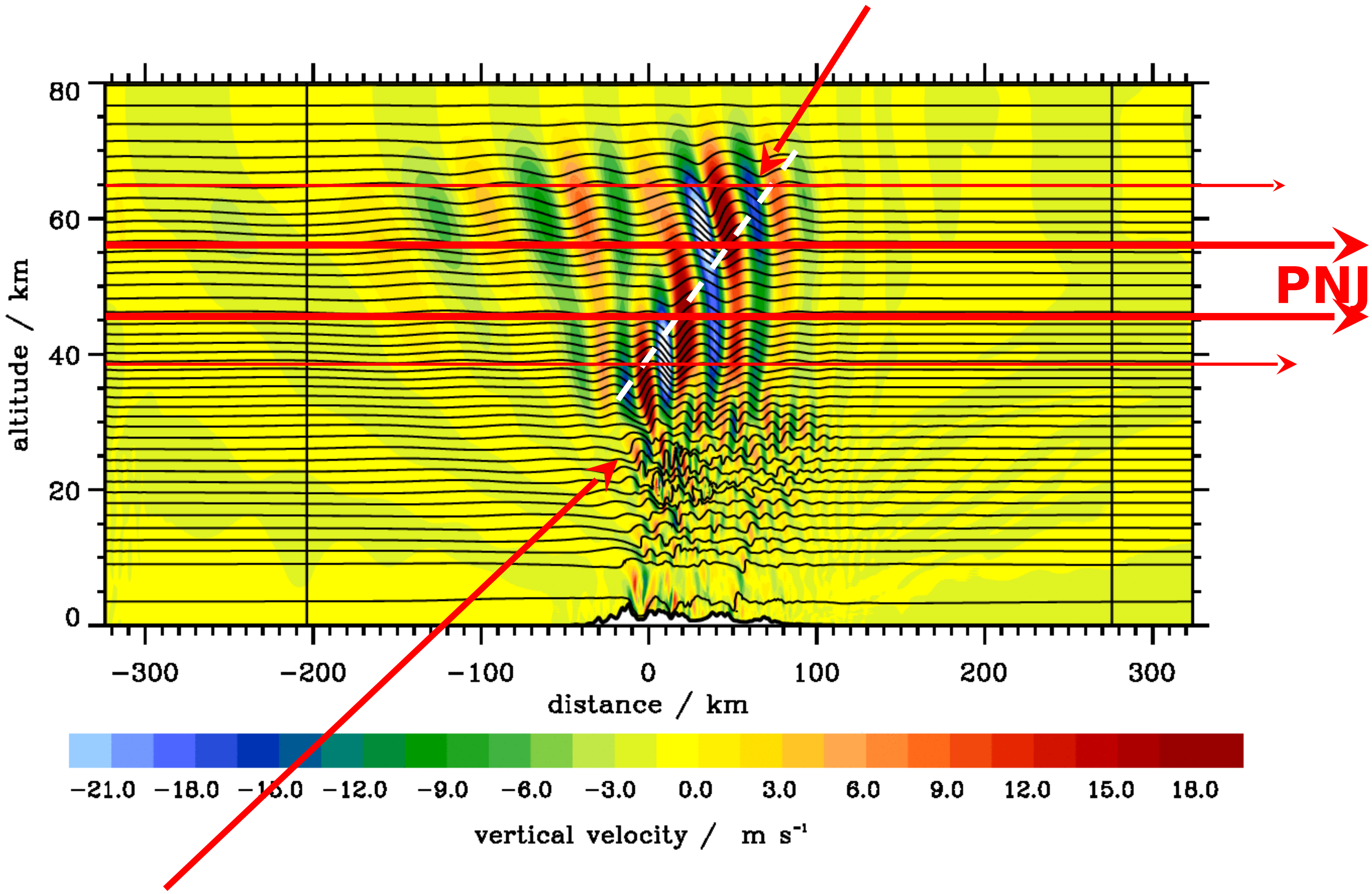

primary breaking region

t = 90 min – excitation of stratospheric wave trains

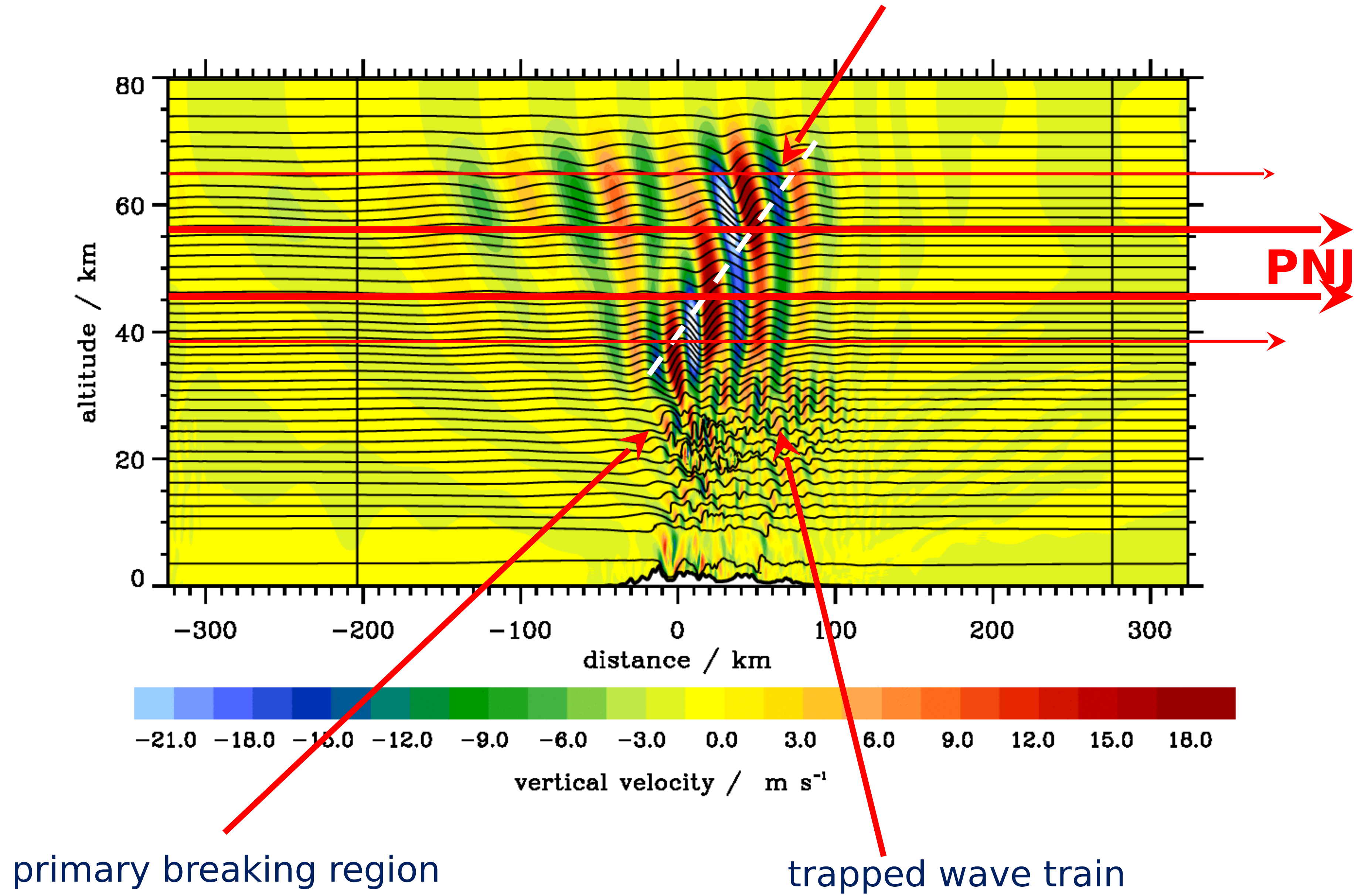

t = 138 min – ceased, almost linear stratospheric wave field

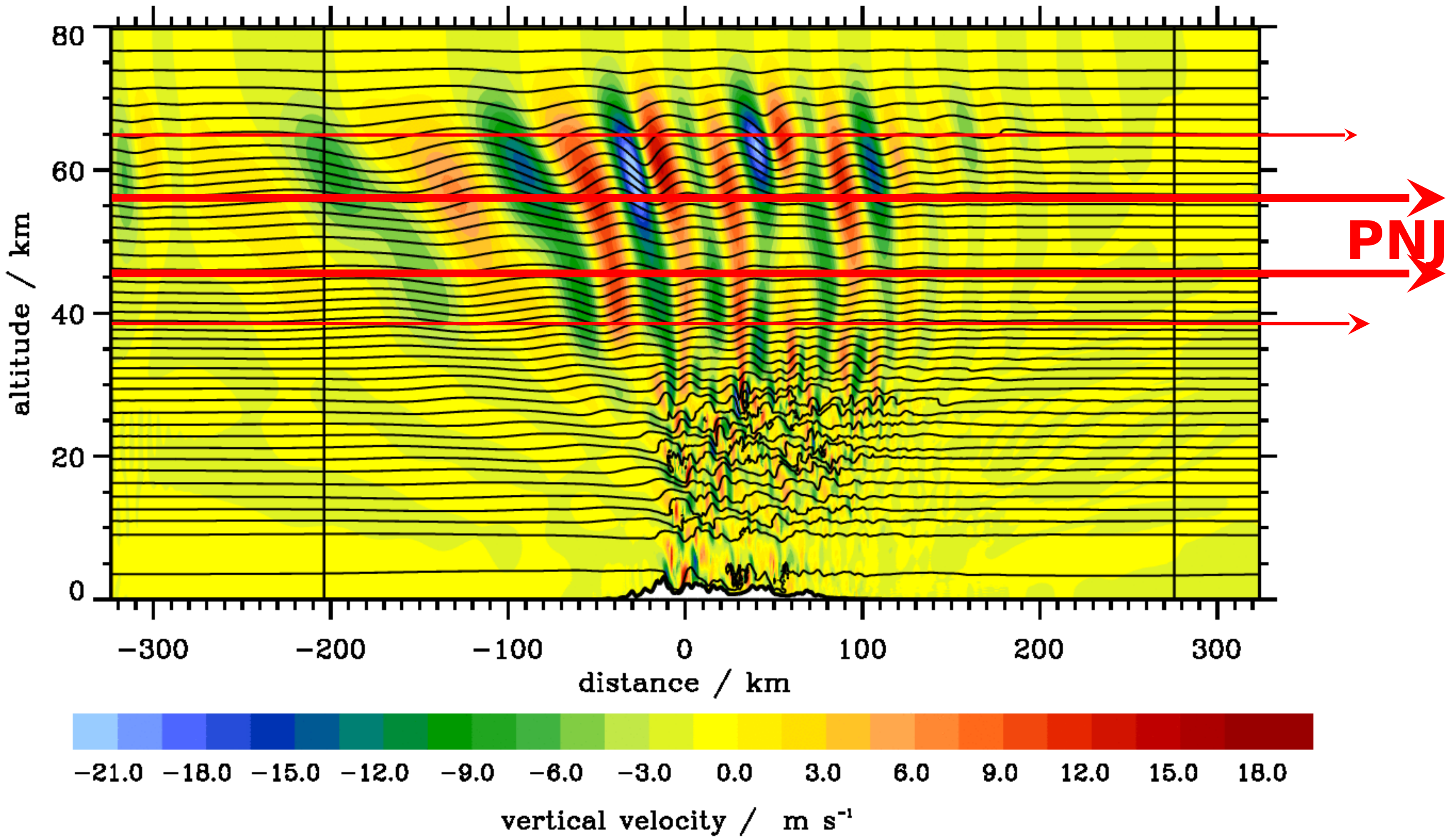

t = 540 min – sporadic appearance of mesospheric rotors

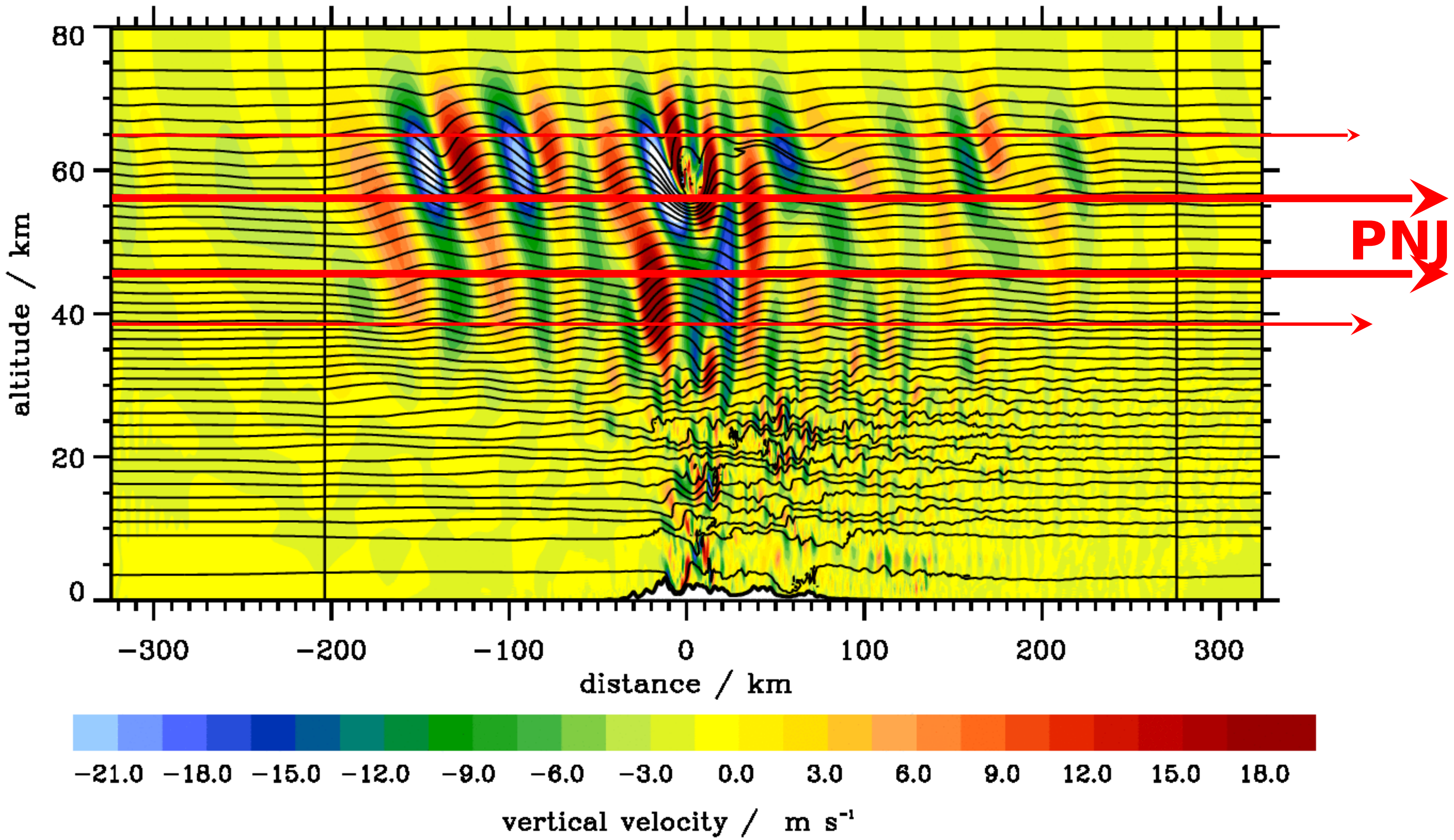

Prusa et al 1989   Bacmeister and Schoeberl 1989

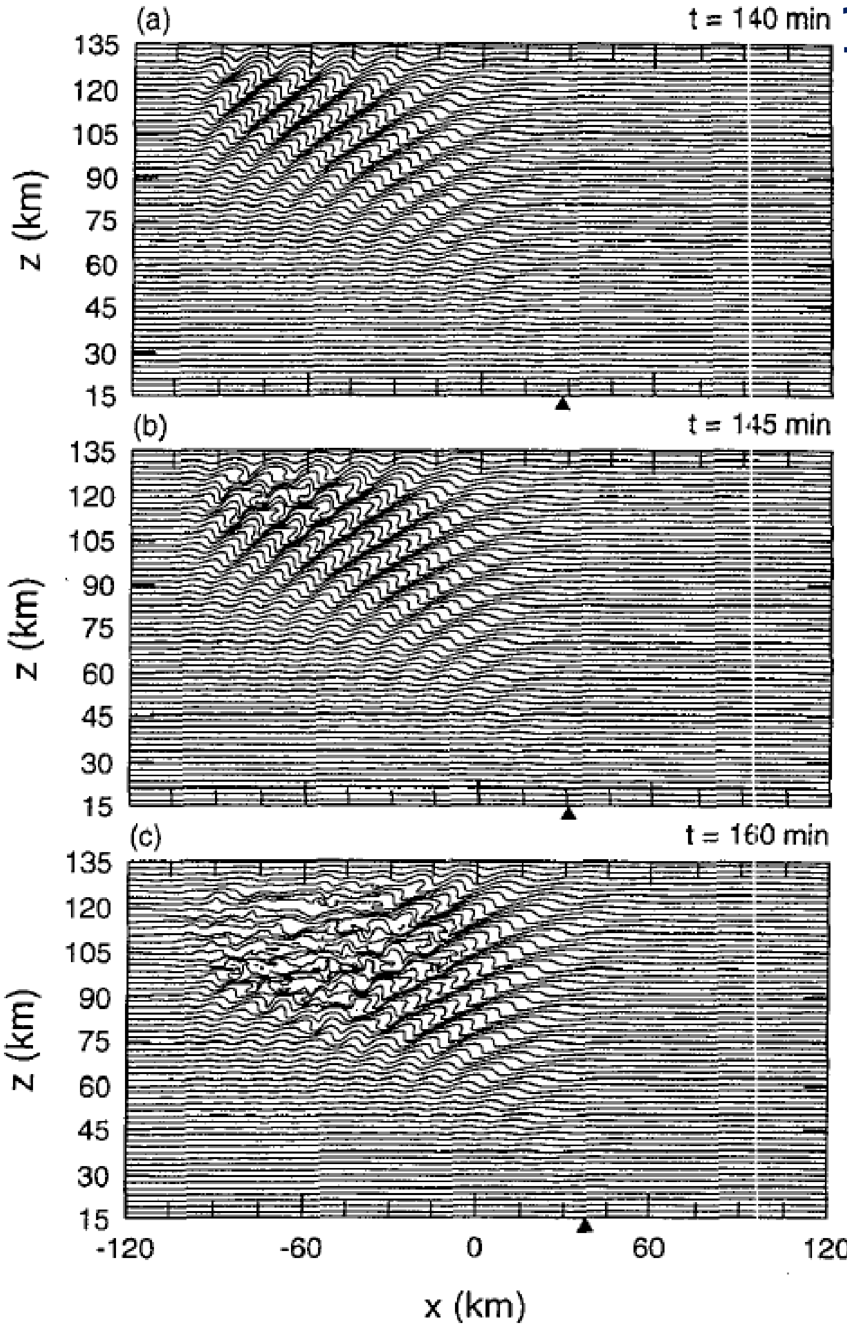

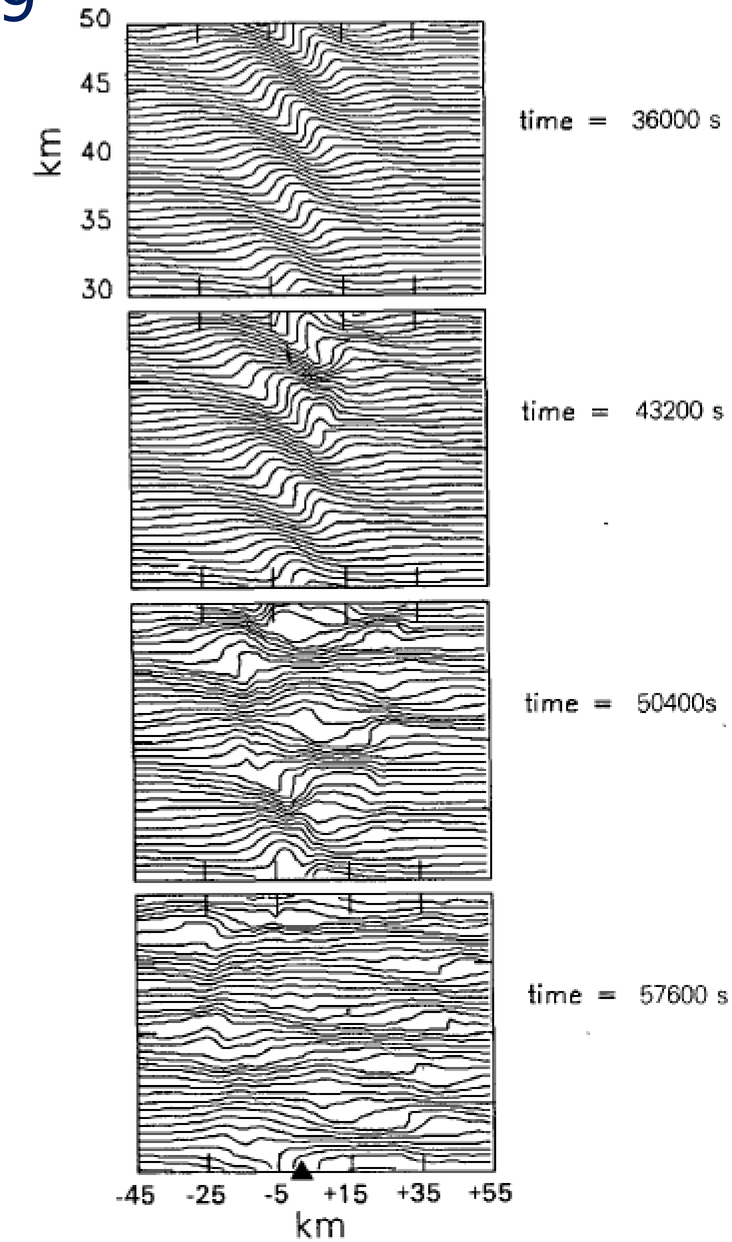

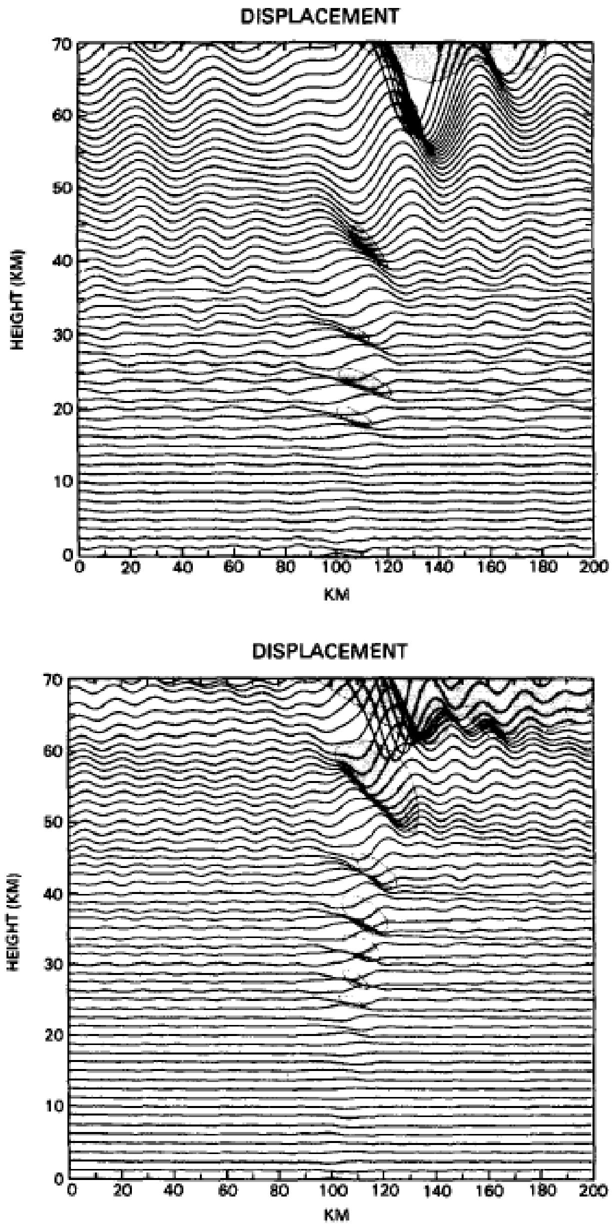

FIG. 2. Particle displacements associated with mountain waves are shown at different altitudes. The mountain is centered at 100 km and is profiled by the lowest displacement line. Panel (a), shows results using the winter wind profile; panel (b), the equinox wind profile. Shaded regions indicate zones where Ri < 1/4.

Schoeberl, M., 1985: The penetration of mountain waves into the middle atmosphere, *J. Atmos. Sci.* **42**, 2856-2864

Simultaneous MLT gravity wave event

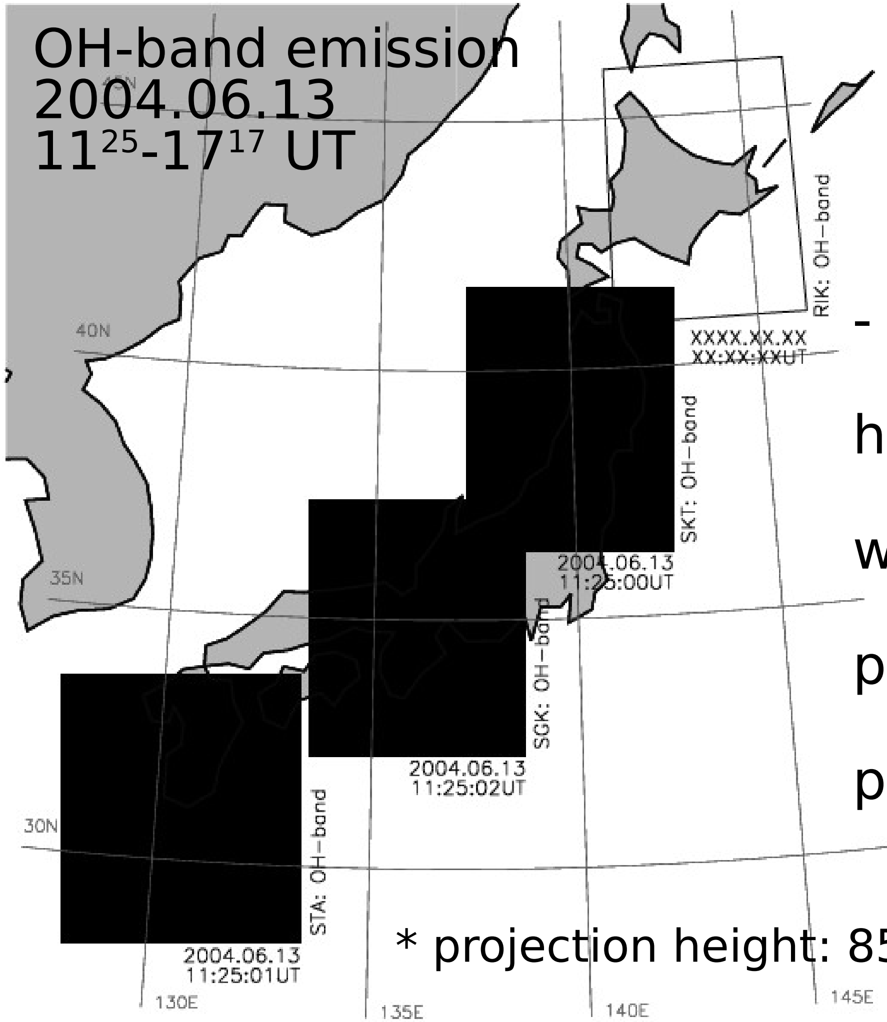

* projection height: 85km

- estimated wave parameters -

horizontal wavelength:	33.4 ±4.9 km
wave period:	13.4 ±2.9 min
phase speed:	42.8 ±7.4 m/s
propagation direction:	Northward
	13.4 ±3.7 deg

S. Suzuki et al., AGU Fall Meeting 2012

Dynamics in the upper stratosphere and mesosphere

- deep vertical propagation of non-hydrostatic gravity waves

- waves trapped in the vicinity of the polar night jet (PNJ) and underneath the stratopause – <u>totally different appearance of wave fronts compared to uniform wind & uniform stability simulations</u>

- horizontally and vertically propagating waves above the PNJ

- sporadic wave breaking between strong up- and downdrafts (mesopheric rotors)

- very rapid change of middle atmospheric wave field in 12 h simulation time

Dynamics in the upper stratosphere and mesosphere

Internal Reflection of gravity waves

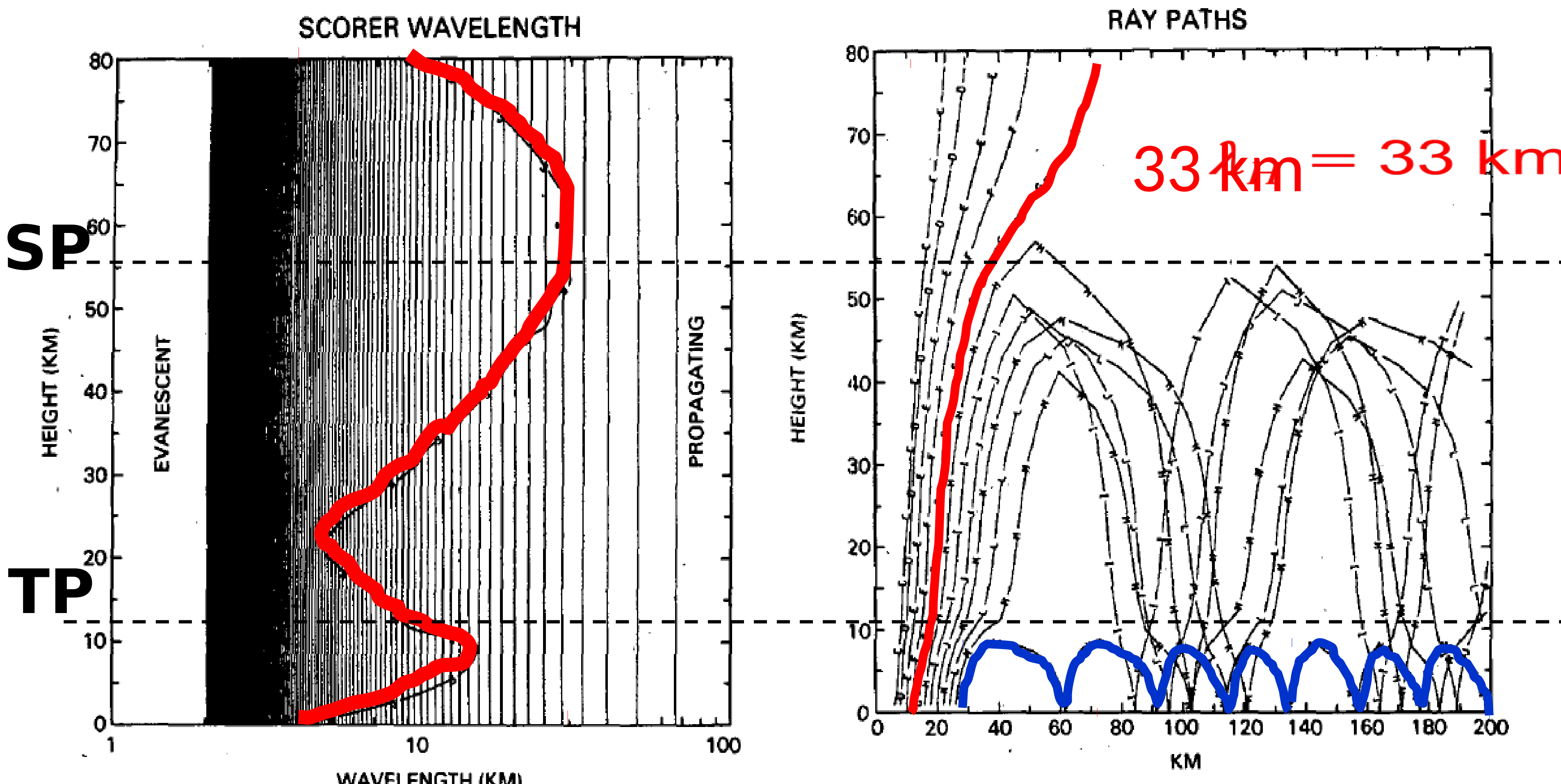

$k > \ell$ $\qquad$ $k < \ell$

$$\lambda_S = \frac{2\pi}{\ell}$$

$\lambda = 15$ km

Schoeberl, 1985

Dynamics in the upper troposphere and lower stratosphere (UTLS)

- analyse rough and smoothed Mt. Cook 1b topography runs:
- show power spectra of u, w, and T at z=12 km along leg 11 of RF05 at one selected time

ECMWF IFS Upstream Profiles 16 June 2016 12 UTC

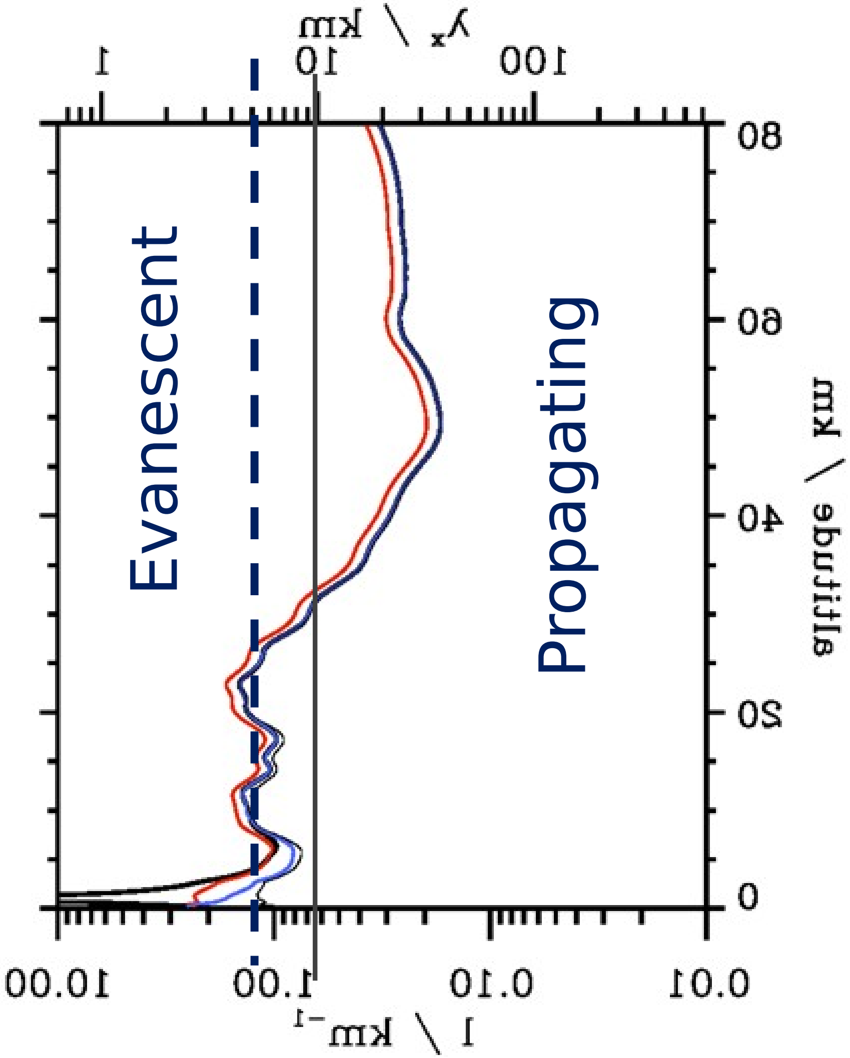

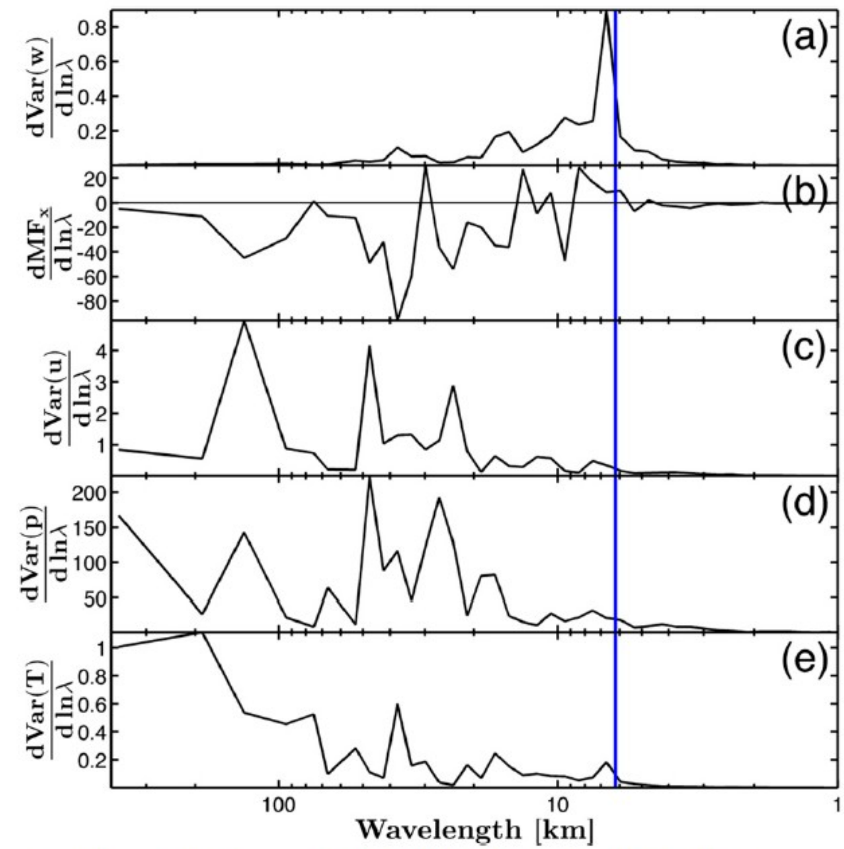

FIG. 9. Aircraft-derived spectra for Mt. Cook flight RF05, leg 11 on 16 Jun 2014: (a) *w* power, (b) MFx, (c) *u* power, (d) *p* power, and (e) *T* power. The vertical blue line is the estimated buoyancy cutoff for this leg. Note the shift in dominant wavelength between (a) and (c)–(e).

thick black line: u **red line**: u_{ROT1} (magnitude of positive $u_{\parallel}$ and $v_{\parallel}$ with 300° along track direction

thin black line: v_H **blue line**: u_{ROT2} (wind direction turns from 320° to 270° in the lowest 10 km)

16 June 2016, Init: 12 UTC (+420 min)
z = 12 km

Mt Cook 1b – Rough EULAG run

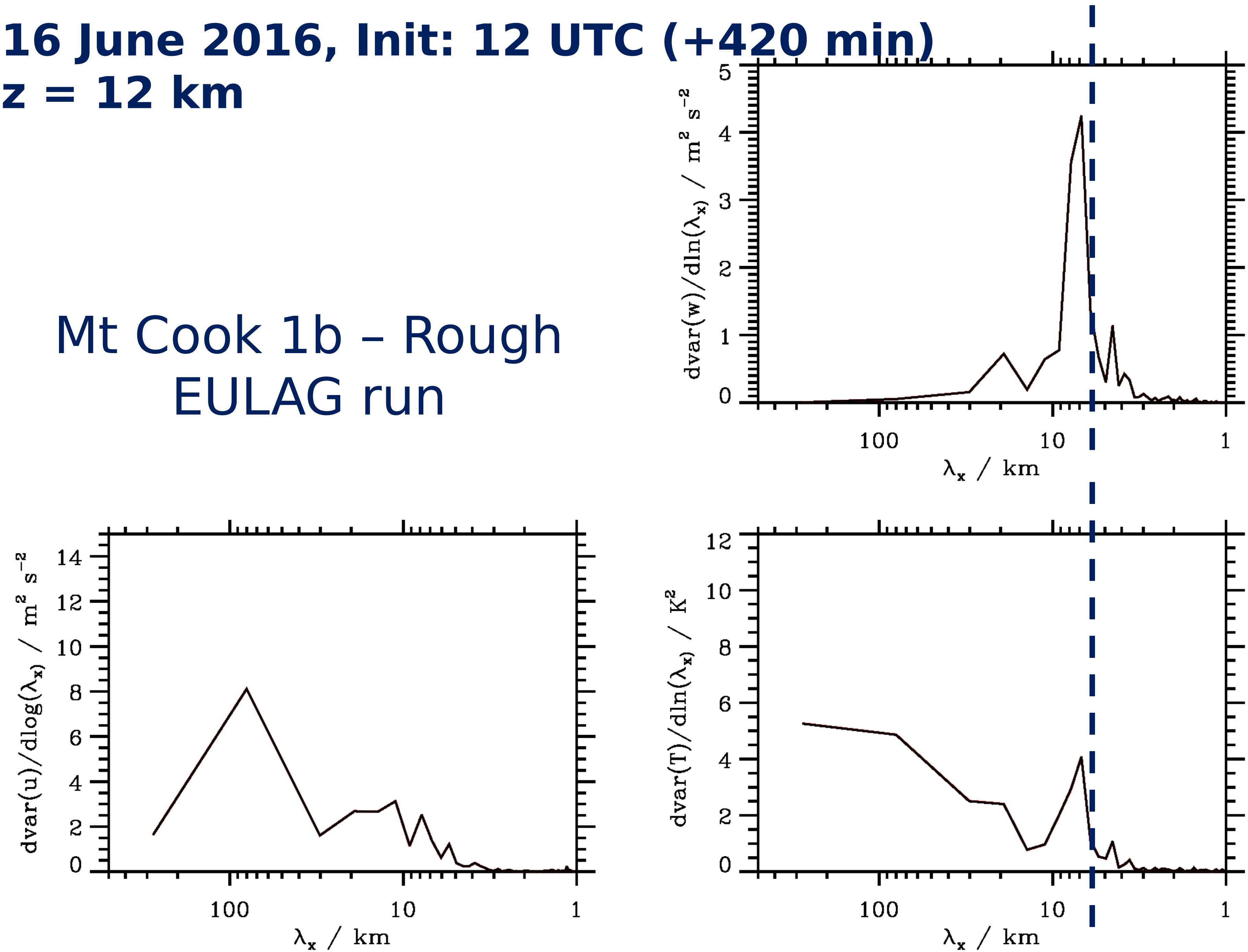

16 June 2016, Init: 12 UTC (+420 min)
z = 30 km

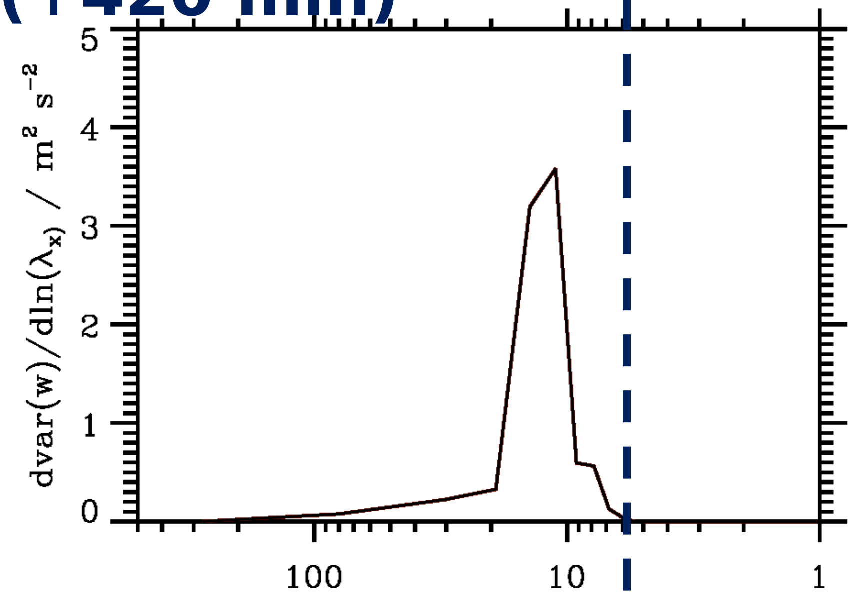

Mt Cook 1b – Rough
EULAG run

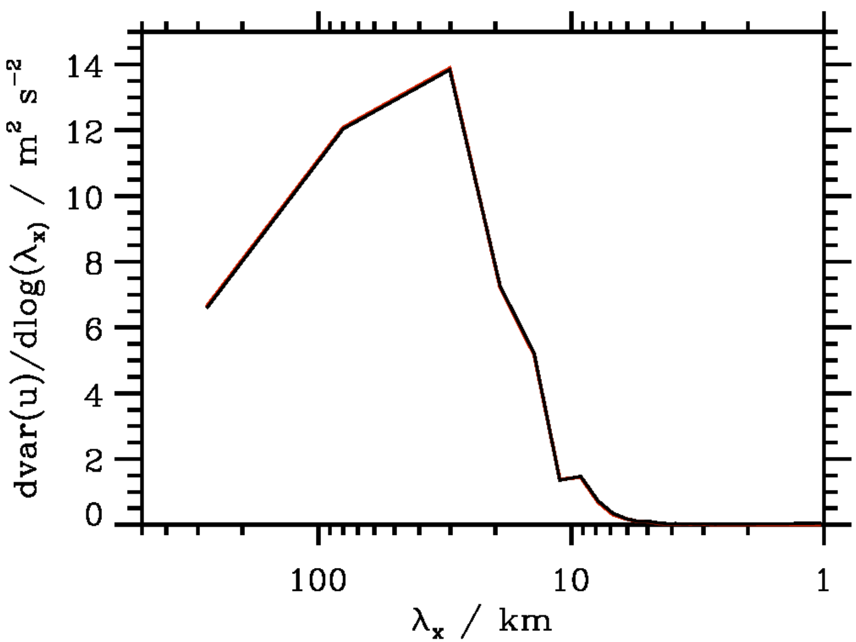

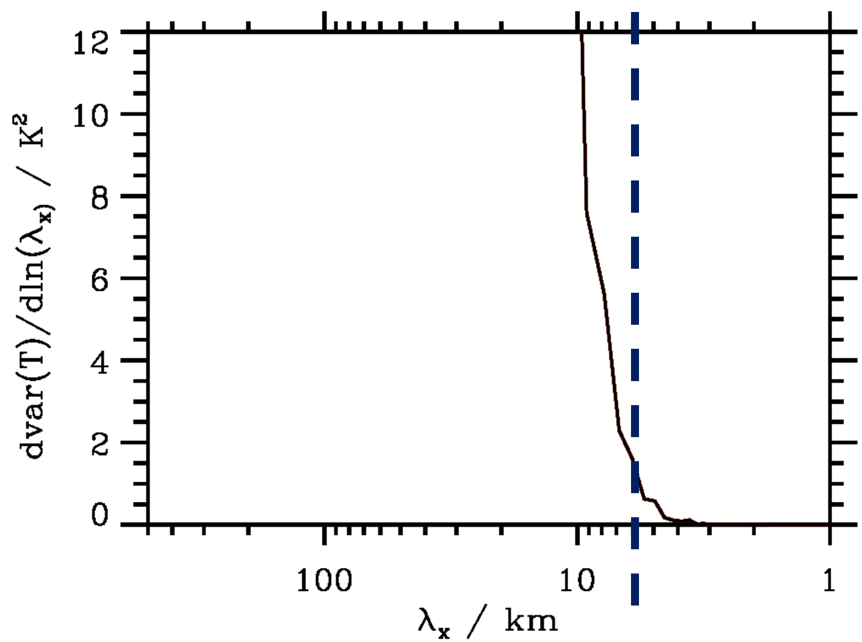

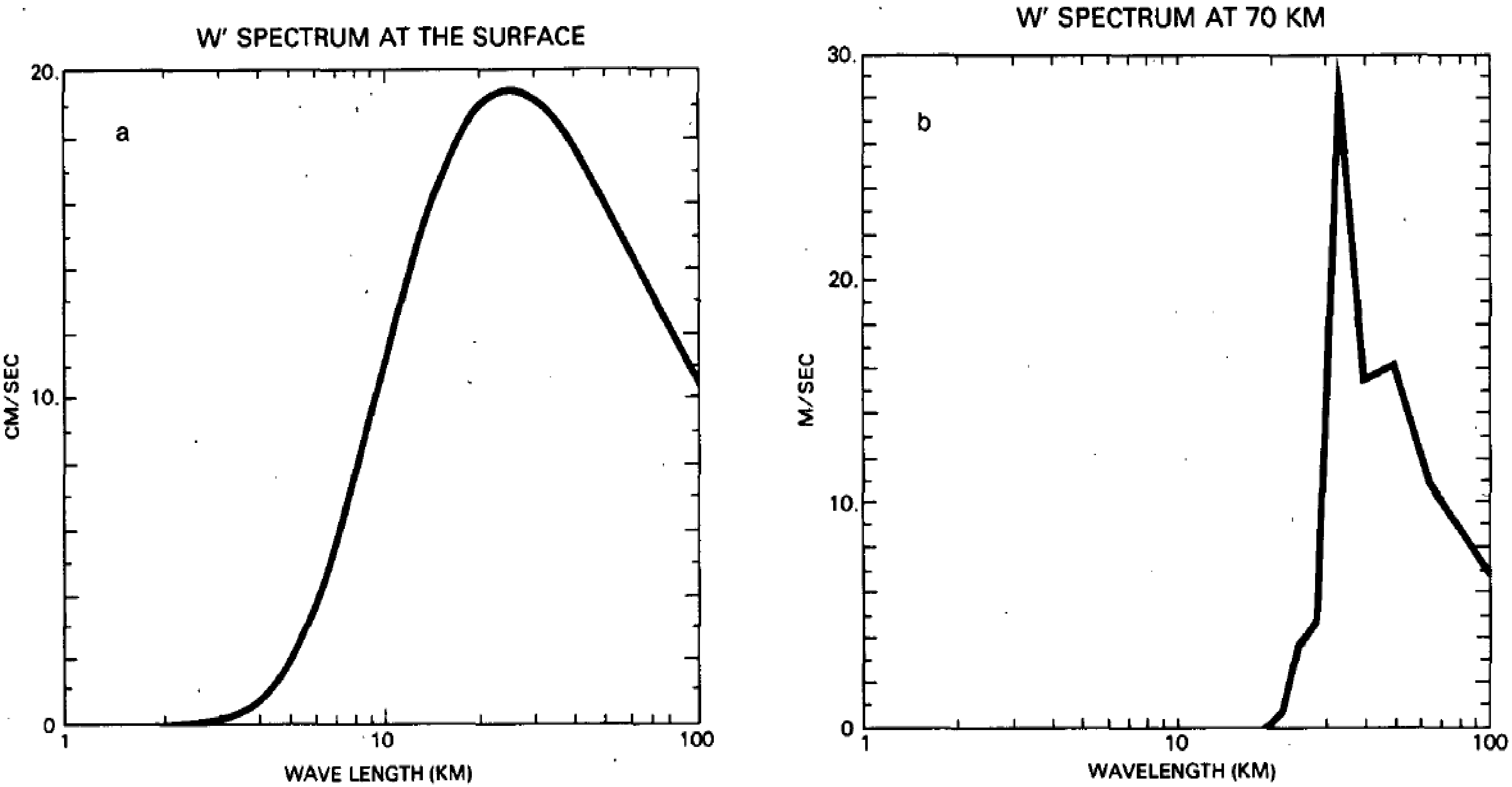

Schoeberl, 1985

What about the roughness of NZ‘s terrain?

Mt Cook 1b

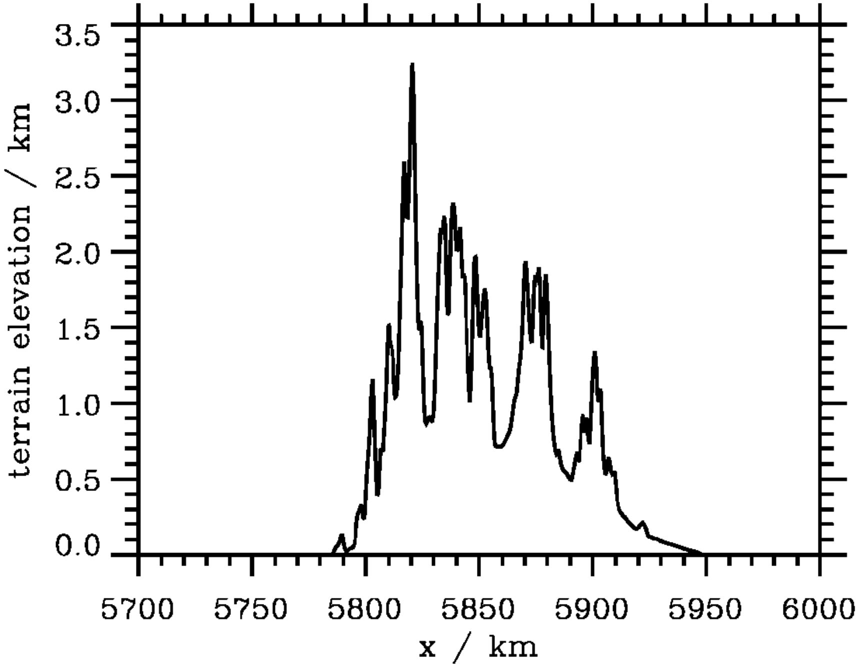

terrain elevation / km
x / km

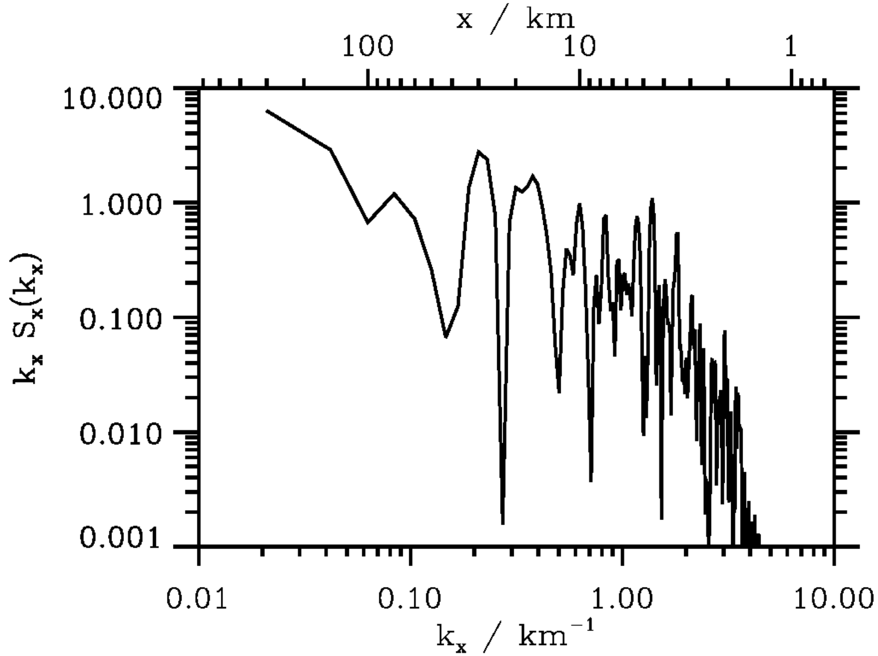

x / km
$k_x S_x(k_x)$
k_x / km^{-1}

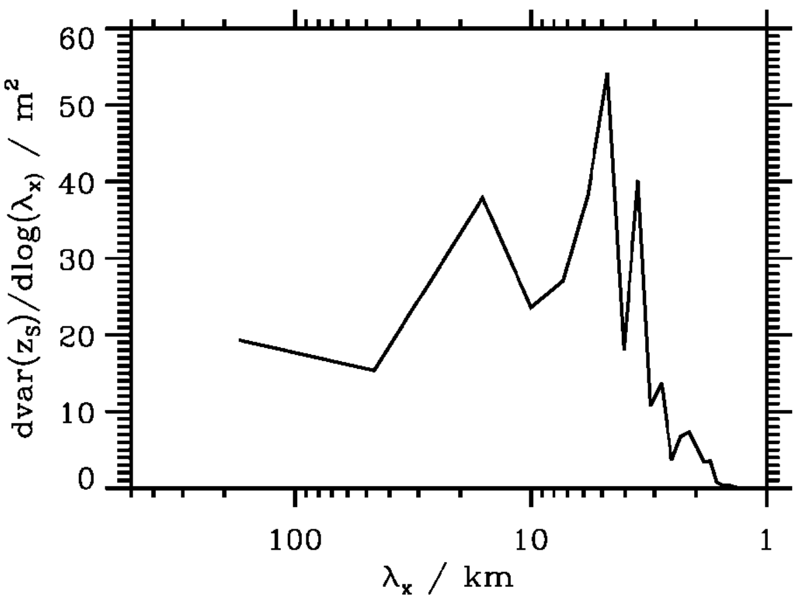

dvar(z_S)/dlog(λ_x) / m^2
λ_x / km

Mt Cook 1b - Smoothed

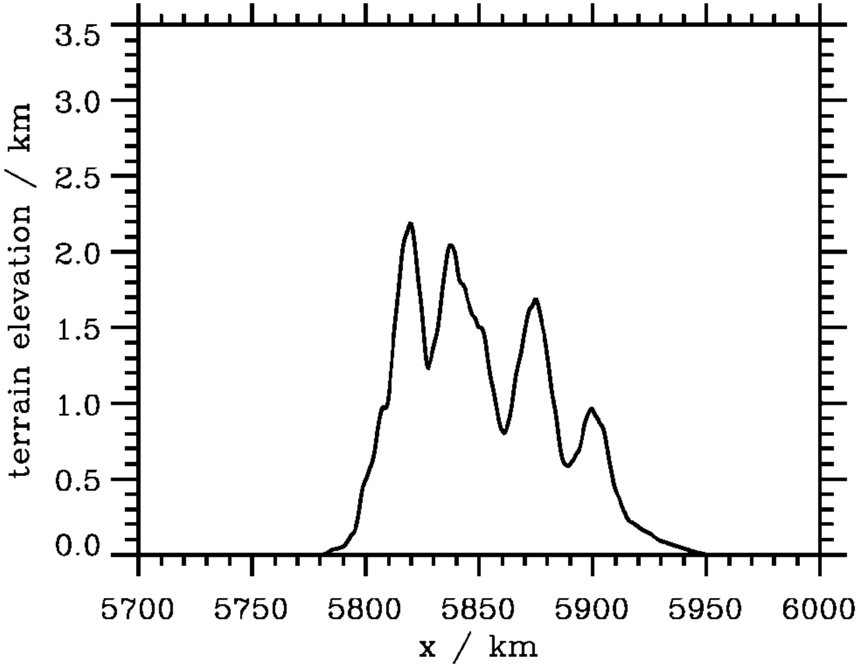

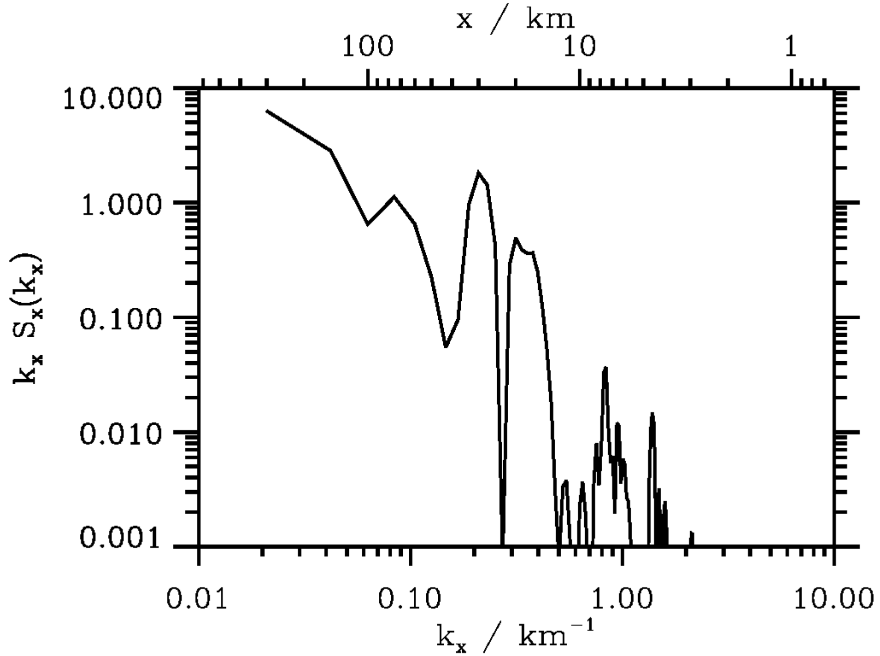

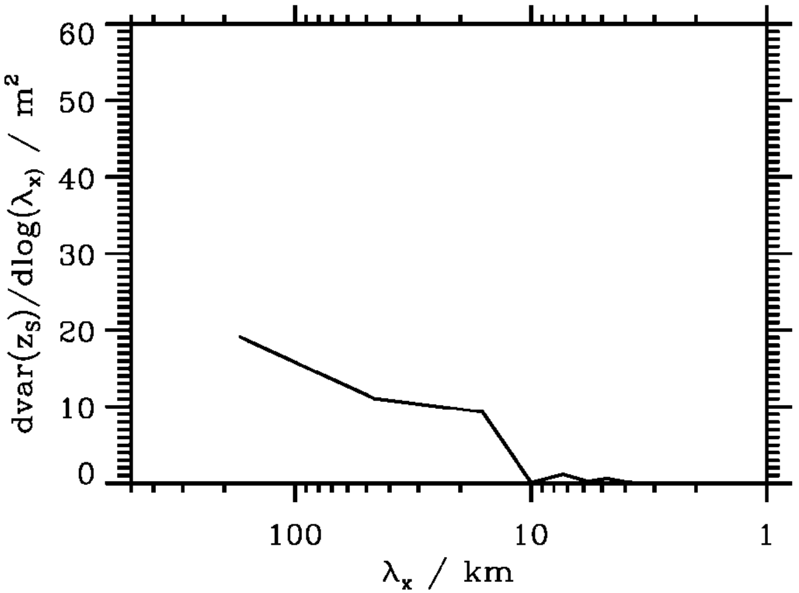

16 June 2016, Init: 12 UTC (+420 min)
z = 12 km

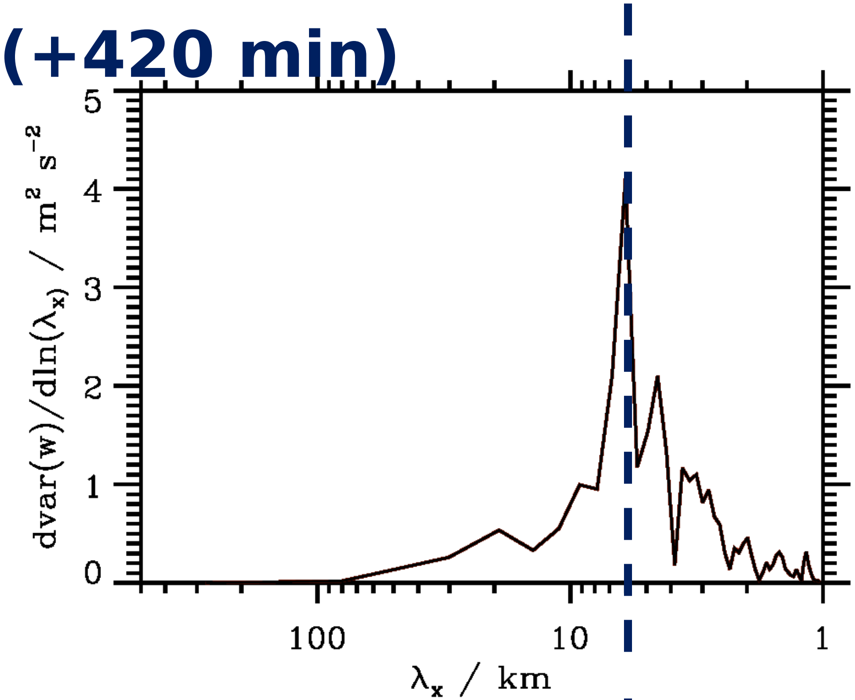

Mt Cook 1b – Smooth EULAG run

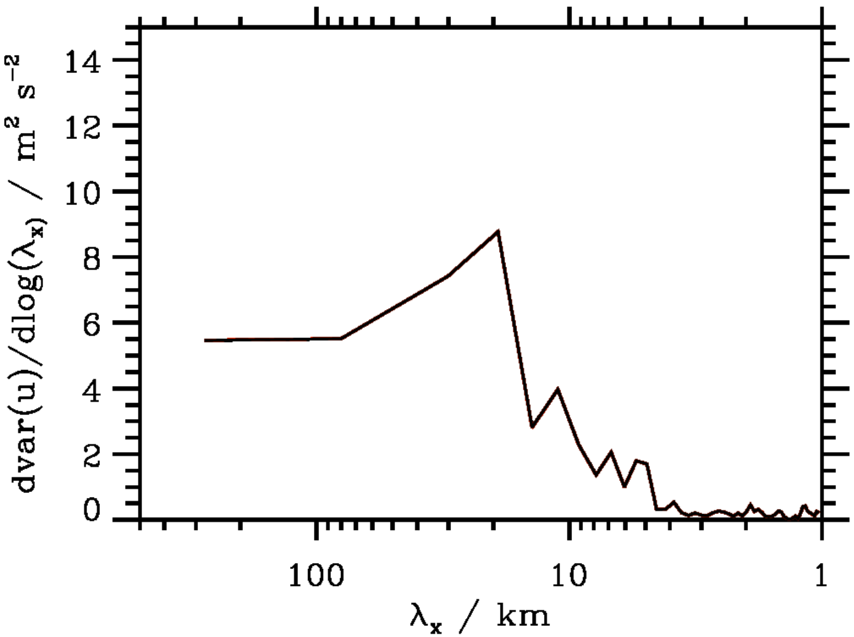

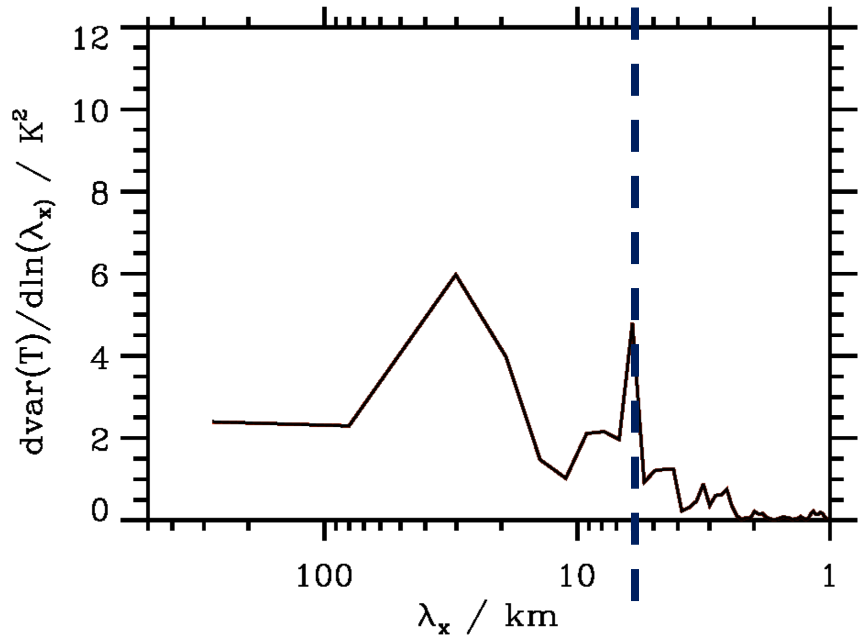

16 June 2016, Init: 12 UTC (+420 min)
z = 12 km

Mt Cook 1b – Rough EULAG run

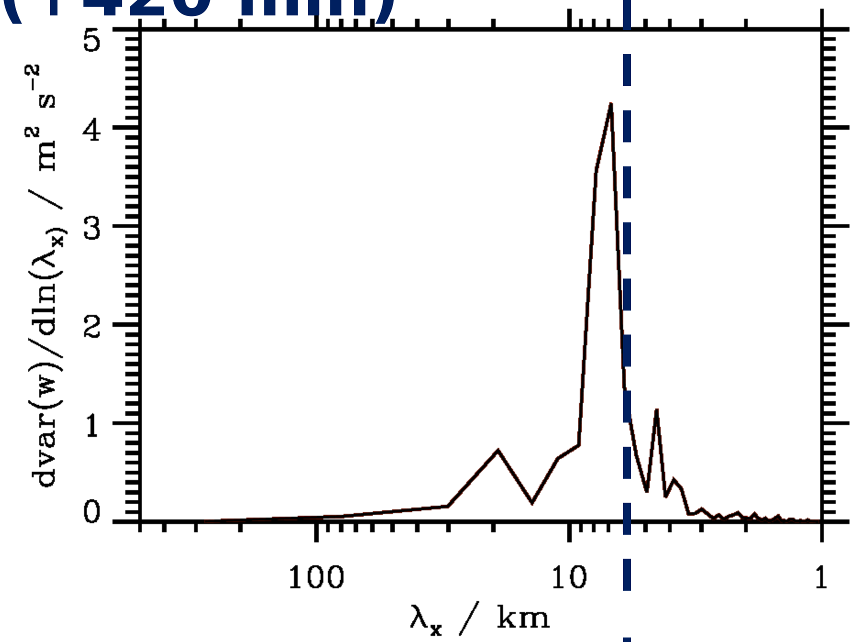

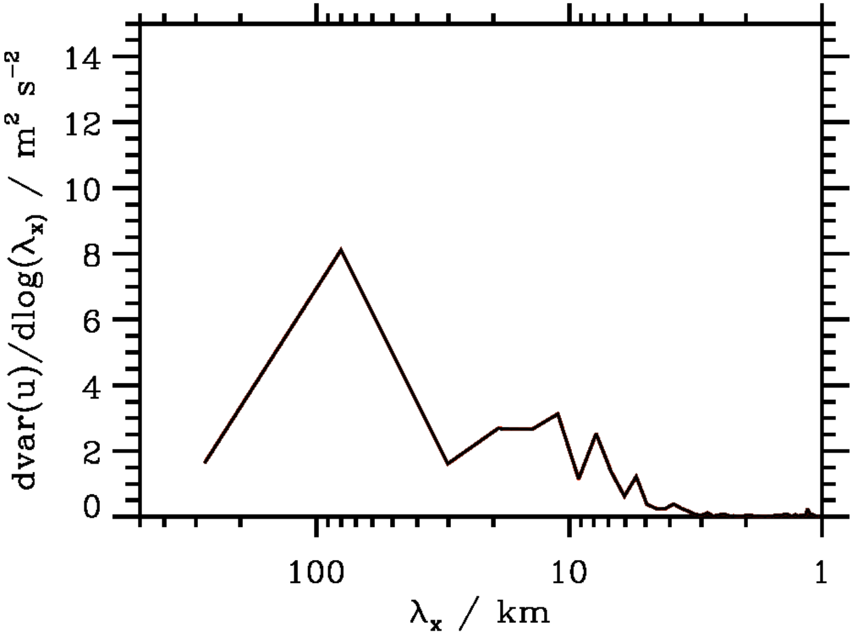

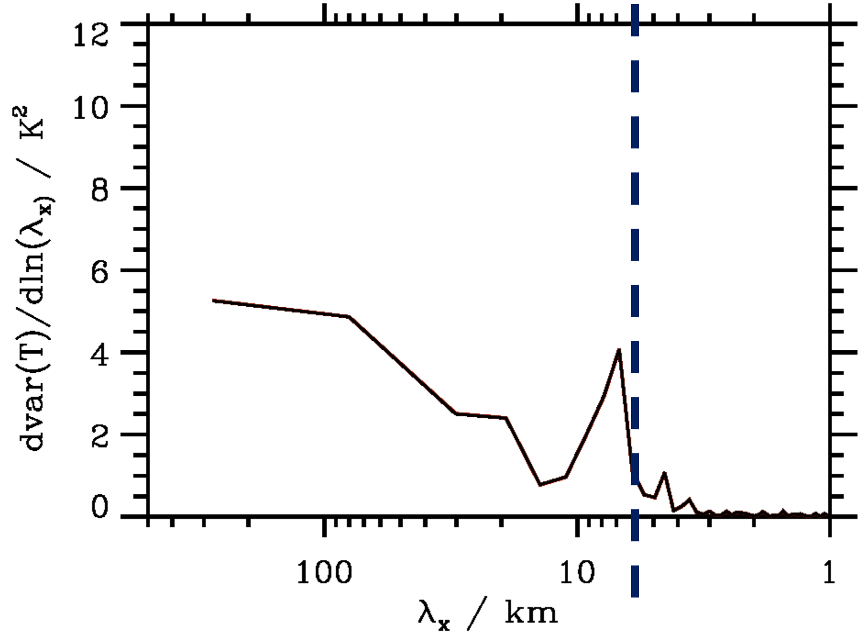

Dynamics in the upper troposphere and lower stratosphere

- EULAG simulations reproduce observed broad mountain wave spectrum with w-peaks at around 7 km (~ cut-off wavelength) and long-wavelength power in u and T

  ➜ observed peaks in the w-spectrum are realizable in high-resolution numerical simulations

- roughness of the terrain does not seem to have an overwhelming impact on the spectra in the UTLS

  ➜ wind filtering dominates the wavelength selection

AND/OR

➜ wave trapping and interference with waves propating up- and downwards through the UTLS are the essential ingredients producing the observed spectra